12-11-2017

Oxygen Isotopic Composition of Nitrate Produced by Freshwater Nitrification

Danielle Boshers
danielle.boshers@uconn.edu

Oxygen Isotopic Composition of Nitrate Produced by Freshwater Nitrification

Danielle Sue Boshers

B.S., University of Michigan, 2015

A Thesis Submitted

in Partial Fulfillment of the

Requirements for the Degree of

Master of Science

At the University of Connecticut

2017

Approval Page

Master of Science Thesis
Oxygen Isotopic Composition of Nitrate Produced by Freshwater Nitrification

Presented by:
Danielle Sue Boshers

Major Advisor _____
Julie Granger, Ph.D.

Associate Advisor _____
Craig Tobias, Ph.D.

Associate Advisor _____
David Lund, Ph.D.

University of Connecticut

2017

Acknowledgements

Foremost, I would like to express my gratitude to my advisor Dr. Julie Granger, whose guidance, dedication, and humor made this research project possible as well as enjoyable. I am eternally grateful for all of the once in a life time opportunities she has given to me to explore not only science, but also the world. This project was also made possible thanks to Dr. John Karl Böhlke from USGS through his guidance and water isotope analysis. I gratefully acknowledge the funding support from the National Science Foundation and UConn's Feng Student Travel Fund for assistance in sending me to AGU to present this research. I would also like to acknowledge all of the technical help that I have received along the way: Claudia Koerting for assistance with nutrient analysis and her unwavering uplifting demeanor, Gregory Cane and David Cady for troubleshooting and fixing the IRMS, our undergraduate work-horse, Reide Jacksin, for help with preparing my samples for isotope analysis, and Rich Dabundo for training me in all things Granger Lab. I am also grateful to my committee members, Craig Tobias and David Lund for their help and guidance. Last but certainly not least, I would like to thank my fiancé Taylor Snow, my family, and my fellow UConn Marine Sciences graduate students for all of their love and encouragement.

Table of Contents

List of Tables and Figures

Abstract

Identifying sources of nitrate (NO_3^-) in the environment is important to elucidate causes of water quality impairment and eutrophication. Measurements of naturally occurring stable isotope ratios of nitrogen ($^{15}N/^{14}N$) and oxygen ($^{18}O/^{16}O$) in NO_3^-, can be used to determine the sources, dispersal, and fate of natural and contaminant NO_3^- in aquatic environments. To this end, it is necessary to know how NO_3^- isotopologues are modified by biological reactions, as heavy and light isotopes have different reaction rates. One important microbial reaction that influences isotope ratios of NO_3^- in the environment is nitrifcation, the biological oxidation of ammonium (NH_4^+) to nitrite (NO_2^-) then NO_3^-, the influence of which is not well understood in freshwater systems. The purpose of this study was to determine the influence of the $\delta^{18}O$ of ambient water on the isotopic composition of NO_3^- produced by freshwater nitrification. Water was collected from two streams in New England during the fall and spring, which were amended with NH_4^+ and with increments of ^{18}O-enriched water, and then monitored the isotopic composition of NO_2^- and NO_3^- produced by natural consortia of nitrifiers. Although oxidation rates differed between the two stream waters, the final $\delta^{18}O$ of NO_3^- produced in both experiments revealed a sensitivity to the $\delta^{18}O$ of water mediated by (a) isotopic equilibration between water and NO_2^- and (b) kinetic isotope fractionation during O-atom incorporation from molecular oxygen and water into NO_2^- and NO_3^-. Our results concur with seawater incubations and nitrifying culture experiments that have demonstrated analogous sensitivity of the $\delta^{18}O$ of nitrified NO_3^- to equilibrium and kinetic O isotope effects (Buchwald et al. 2012). These findings have important implications for interpretations of O isotopes in NO_3^- source apportionation studies.

1. Introduction

Human activity has greatly altered the nitrogen cycle, particularly in terrestrial, aquatic and coastal ecosystems, through fossil fuel combustion, use of industrial nitrogen fertilizer, and the release of nitrogen in wastewater. Reactive nitrogen fixed industrially by the Haber Bosch process now rivals that introduced to the biosphere by biological nitrogen fixation (Galloway et al., 2004). The release of reactive nitrogen has resulted in deterioration of groundwater quality, and in eutrophication of freshwater, estuaries, and shelf seas around the globe.

Identifying sources of nitrate (NO_3^-) in the environment is important to elucidate causes of water quality impairment and eutrophication. Measurements of naturally occurring stable isotope ratios of nitrogen ($^{15}N/^{14}N$) and oxygen ($^{18}O/^{16}O$) in NO_3^-, can be used to determine the sources, dispersal, and fate of natural and contaminant NO_3^- in aquatic environments. Henceforth we express isotope ratios in "delta" notation, where;

$$\delta^{15}N = \left[\left(\frac{^{15}N}{^{14}N}\right)sample \div \left(\frac{^{15}N}{^{14}N}\right)air - 1\right] \times 1000$$

$$\delta^{18}O = \left[\left(\frac{^{18}O}{^{16}O}\right)sample \div \left(\frac{^{18}O}{^{16}O}\right)VSMOW - 1\right] \times 1000$$

To use NO_3^- isotopes in this way, it is necessary to know the extent to which NO_3^- isotopologues, molecules that differ only in their isotopic composition, are influenced by biological reactions that produce and consume NO_3^-, as heavy and light isotopologues can have different reaction rates during biological transformations. Small differences in respective reaction rates (*k*) can result in notable isotope fractionation between reactant and product

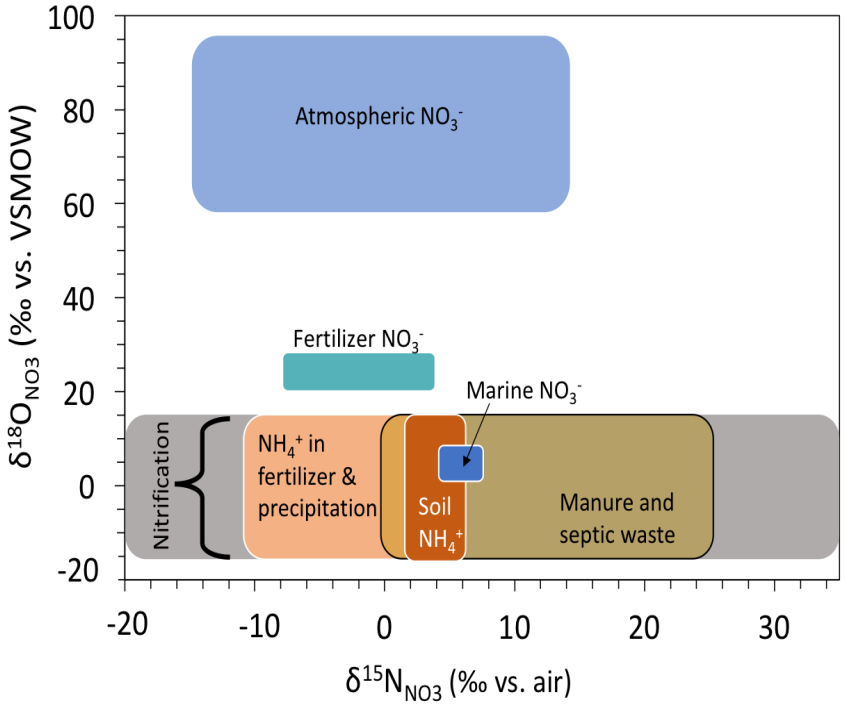

Figure 1. Typical values for $\delta^{15}N$ and $\delta^{18}O$ NO_3^- associated with, or nitrified from, various N sources to freshwaters. Adapted from Kendall et al. 2007.

pools. The extent to which heavy and light isotopologues are fractionated during a unidirectional chemical reaction is described by kinetic isotope effects, ε, where ${}^{heavy}\varepsilon_k$ (‰) = $({}^{light}k/{}^{heavy}k - 1) \times 1000$ (Mariotti et al., 1981).

One important microbial reaction that influences isotope ratios of NO_3^- in the environment is nitrification, the biological production of NO_3^- from the oxidation of ammonium (NH_4^+) to nitrite (NO_2^-) then NO_3^-. This process is carried out bacteria and archaea that use NH_4^+ (as ammonia, NH_3) and NO_2^- as respective reductants to chemosynthesize organic carbon from carbon dioxide (CO_2). In the environment, NO_3^- produced by nitrification can be distinguished from other sources, namely from atmospheric deposition or industrial fertilizers, based on its $\delta^{18}O_{NO3}$ composition (Fig. 1). NO_3^- produced by nitrification typically has a comparatively low $\delta^{18}O$ relative to atmospheric and fertilizer NO_3^-, which is assumed to derive from the fractional contribution of O atoms originating from O_2 (~24.2‰; Kroopnick & Craig, 1972) and water (-10 to 0‰) during the biological oxidation of NH_4^+ to NO_3^-. Indeed, a culture study of NH_4^+ oxidizing bacteria using ${}^{18}O_2$ and $H_2{}^{16}O$ enriched medium revealed that one O atom is first incorporated from O_2 to produce hydroxylamine (NH_2OH) followed by a second

oxygen atom incorporation from H_2O to produce NO_2^- (Andersson & Hooper, 1983). A parallel study using NO_2^- oxidizing bacteria with experimental treatments of $H_2{}^{18}O$, $^{18}O_2$, or $P^{18}O_4$ enriched media demonstrated that the third O atom incorporated into NO_3^- is sourced from water (Kumar et al., 1983). The $\delta^{18}O_{NO3}$ estimated from the fractional source contribution of O atoms (Eqs. 1 and 2) has thus provided a benchmark from which to identify the contribution of nitrified NO_3^- in the environment (Amberger & Schmidt, 1987; Voerkelius et al., 1990; Durka et al., 2004).

$$\delta^{18}O_{NO2,nitrified} = \frac{1}{2}\left(\delta^{18}O_{H2O}\right) + \frac{1}{2}\left(\delta^{18}O_{O2}\right) \quad (1)$$

$$\delta^{18}O_{NO3,nitrified} = \frac{2}{3}\left(\delta^{18}O_{H2O}\right) + \frac{1}{3}\left(\delta^{18}O_{O2}\right) \quad (2)$$

By this convention, the $\delta^{18}O_{NO3}$ produced by nitrification in systems where the $\delta^{18}O$ of water ranges from -10 to 0‰ should range between 1.4 and 8.1‰, assuming a $\delta^{18}O$ for molecular O2 of ~24.2‰ (Kroopnick & Craig, 1972). However, a number of observations from soil incubation experiments suggest that the $\delta^{18}O$ of nitrified NO_3^- may not conformed to the model described by Eq. 2. Amberger and Schmidt, 1987 and Voerkelius et al., 1990 reported negative $\delta^{18}O$ values for nitrified NO_3^-, whereas others reported values greater than expected from Eq. 2. (Burns & Kendall, 2002; Mayer et al., 2001; Spoelstra et al., 2007). Values of $\delta^{18}O$ of nitrified NO_3^- lower than expected from Eq. 2 have been ascribed to a biologically mediated exchange of O atoms between NO_2^- and H_2O during NH_4^+ oxidation (Andersson et al., 1982; Andersson & Hooper, 1983; Fang et al., 2012; Snider et al., 2010). Values greater than expected $\delta^{18}O$ for nitrification were attributed to O isotopic enrichments of H_2O and O_2 due to evaporation and respiration.

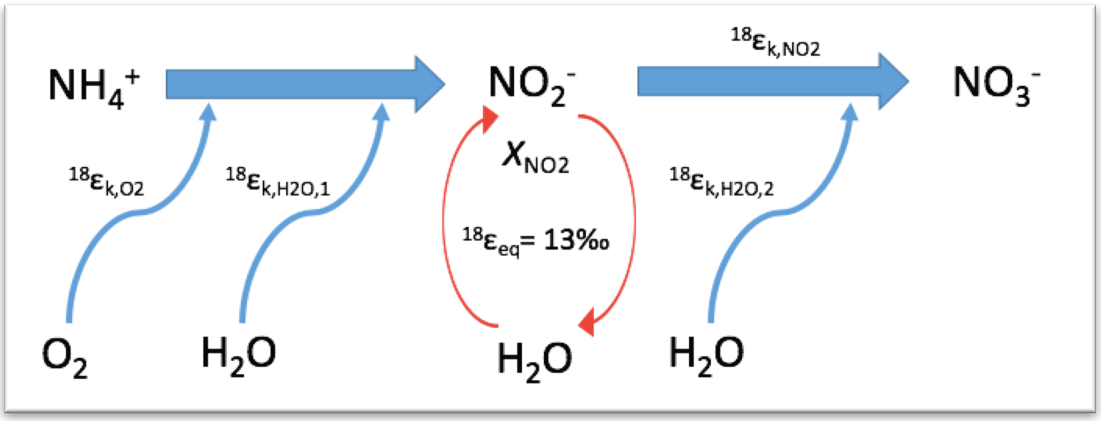

Figure 2. Schematic of O isotopic fractionation and exchange during nitrification (reproduced from Casciotti et al. 2012). Sources of O atoms (O_2 and H_2O) for NH_3 and NO_2^- oxidation are shown, as well as predicted isotope effects for NO_2^- oxidation ($^{18}\varepsilon_{k,NO2}$), oxygen atom incorporation ($^{18}\varepsilon_{k,O2}$, $^{18}\varepsilon_{k,H2O,1}$, and $^{18}\varepsilon_{k,H2O,2}$) and exchange ($^{18}\varepsilon_{eq}$). Also shown is the fractional exchange of NO_2^- O atoms that have been equilibrated with H_2O.

Mayer et al. 2001 also suggests that only one-third of the oxygen in nitrified NO_3^- was derived from water in a coniferous soil incubation, which they attribute to purported heterotrophic nitrification – in which two of the three O atoms in NO_3^- are allegedly derived from an organic nitrogen compound and only one from water (Wood 1988; Wood 1990; Hollocher 1984). The heterogeneity among observations and explications of observed trends reflect a lack of fundamental understanding of the $\delta^{18}O$ variations produced by nitrification, which leads to uncertainty in interpretations of $\delta^{18}O$ signatures of NO_3^- in freshwater environments.

Recent evidence from cultures and field incubations, however, reveal that $\delta^{18}O_{NO3}$ is sensitive not only to $\delta^{18}O$ composition of water incorporated, but also to kinetic and equilibrium isotope effects. (Figure 2). The respective incorporations of O atoms from molecular O_2 and water during NH_4^+ oxidation by cultures of bacterial and archaeal isolates from marine and terrestrial systems are associated with substantial isotope effects ($^{18}\varepsilon_{k,H2O,1}$ and $^{18}\varepsilon_{k,O2}$), on the order of 18 to 38‰ combined (i.e. $^{18}\varepsilon_{k,H2O,1}$ + $^{18}\varepsilon_{k,O2}$; Casciotti et al. 2010; Buchwald et al. 2012). Culture work also revealed a pH- and temperature-dependent tendency for biologically enhanced O atom exchange between NO_2^- and H_2O during NH_4^+ oxidation (0 –

25% of O atoms exchanged over 2 days), with an associated equilibrium isotope effect of ~13‰ (Casciotti et al. 2007; Casciotti et al. 2010; Figure 2).

Culture studies on marine NO_2^- oxidizing bacteria have also revealed a role for incorporation and kinetic isotope effects during NO_2^- oxidation to NO_3^-. For one, the two O atoms of NO_2^- are subject to an inverse kinetic isotope effect upon conversion to NO_3^- ($^{18}\varepsilon_{k,NO2}$), thus causing a depletion of ^{18}O in the NO_2^- pool during oxidation (Casciotti 2009; Buchwald and Casciotti 2010). Another substantial isotope effect was observed in association with O atom incorporation from water into NO_3^- ($^{18}\varepsilon_{k,H2O,2}$), ranging from 9‰ to 25‰ (Buchwald and Casciotti 2010; Buchwald et al. 2012; Figure 2).

In order to determine if insights from culture studies are pertinent to environmental isotope dynamics, Buchwald et al. 2012 investigated the $\delta^{18}O$ value of NO_3^- produced by co-cultures of NH_4^+ oxidizing archaea or NH_4^+ oxidizing bacteria and NO_2^- oxidizing bacteria, as well as by incubations of natural marine assemblages. Examination of the $\delta^{18}O$ of NO_2^- and NO_3^- produced by co-culture and during seawater incubations revealed O atom incorporation isotope effects and NO_2^- isotopic equilibration analogous to those observed in monocultures. The results suggest the $\delta^{18}O$ of newly produced NO_3^- in the ocean (when $\delta^{18}O_{H2O}$ = 0‰ and $\delta^{18}O_{O2}$ = 23.5‰) most likely lies between -1.5‰ and 1.3‰, much lower than the 8.1‰ suggested by Eq. 2.

Accurate interpretation of isotope distribution in the environment requires a sound mechanistic understanding on factors influencing the isotope composition of NO_3^- produced by nitrification. While isotope effects and NO_2^- equilibration with water have been adroitly documented in monocultures and in incubations of seawater communities, these factors are

often disregarded in studies of freshwater environments. Neglecting exchange and isotope effects can lead to an overestimation of nitrification as a source of NO_3^- in source apportioning studies. The purpose of this study is to determine the influence on the $\delta^{18}O$ of ambient water on the isotope composition of NO_3^- produced during nitrification in freshwater systems. In particular, we aim to determine whether the $\delta^{18}O_{NO3}$ produced by a natural consortium of freshwater nitrifiers can be described by fractional source contribution (Eq. 2) or if isotope effects and/or NO_2^- equilibration need to be considered. In doing so, we aim to bridge the gap between interpretations of the $\delta^{18}O_{NO3}$ produced by nitrification in marine and culture nitrification vs. freshwater.

2. Methods

In order to gauge the potential influence of isotope effects and NO_2^- equilibration on the oxygen isotope composition of NO_3^- produced by natural communities of nitrifiers, we incubated stream water in incremental $\delta^{18}O_{H2O}$ treatments. The evolution of N species and their O isotope composition was monitored as NH_4^+ was oxidized sequentially from NH_4^+ to NO_2^- and then NO_3^-, following a protocol analogous to Buchwald et al. 2012 for incubations of natural seawater consortia. Briefly, 40 L of stream water was collected from 2 freshwater streams in coastal Connecticut, in acid-washed 20 L plastic (polypropylene) carboys. The first sampling took place during the Fall of 2016 and will be referred to as Experiment 1, the second sampling occurred in the Spring of 2017 and will be referred to as Experiment 2. Within a few hours of collection, water was returned to the lab and homogenized into one large 50 L, spigoted carboy. A multi-layered coarse mesh was attached to the spigot to filter out large particles as

the water was dispensed into twelve acid-washed, sterile, 2 L glass media bottles. Each bottle was amended with NH_4Cl to obtain a concentration of 50 μmol L^{-1}. The $\delta^{18}O_{H2O}$ of each was adjusted in triplicate bottles by adding increasing amounts of 97-atom-% ^{18}O-labeled water (Cambridge Isotope Laboratories; OLM-240-97) to obtain respective $\delta^{18}O_{H2O}$ treatments described by Table 1. $\delta^{18}O_{H2O}$ treatments for Experiment 1 all fall within the range of natural abundance water isotopes. The dynamic range of $\delta^{18}O_{H2O}$ treatments was broadened for Experiment 2 in order to obtain more accurate estimates of potential isotope dynamics. Bottles were then loosely capped and incubated in the dark at ambient room temperature. Each bottle was subsampled weekly until the first appearance of NO_2^-, and then quasi daily until complete conversion of NH_4^+ to NO_3^-. Samples for nutrient concentration and NO_3^- isotope analysis were frozen immediately upon collection until analysis. Samples for NO_2^- isotope analysis were processed within an hour of collection for Experiment 1 (described below), and preserved with 1M sodium hydroxide and stored frozen pending isotope analysis for Experiment 2.

Table 1. $\delta^{18}O_{H2O}$ among treatments

Treatment	Experiment 1 $\delta^{18}O_{H2O}$ (‰)	Experiment 2 $\delta^{18}O_{H2O}$ (‰)
1	-6.9	-2.2
2	-6.6	3.8
3	-5.5	14.6
4	-4.2	34.0

2.1 DIN analyses --- Nutrient concentrations (NO_3^-, NO_2^-, NH_4^+) were analyzed using standard protocols adapted for automated measurements on a SmartChem® nutrient analyser, a discrete nutrient auto-analyzer (Unity Scientific, Brookfield, Connecticut)[7]. NH_4^+ concentrations were

determined via the Berthelot reaction, the colorimetric reaction of NH_4^+ with alkaline phenol, hypochlorite, and sodium nitroprusside (Zhang et al. 1997). NO_2^- was determined through formation of a reddish purple azo dye produced at a pH of 2.0 to 2.5 by coupling diazotized sulfanilamide with N-(1-naphthyl) ethylenediamine dihydrochloride (NED dihydrochloride). The highly colored azo dye is measured colorimetrically at 550 nm. NO_3^- was determined by reduction to NO_2^- by passage of a sample through an open tubular copperized cadmium reactor. The resulting NO_3^- plus NO_2^- are measured via the same protocol for NO_2^- above. (Zhang et al. 1997). Some NO_2^- and NO_3^- concentrations were measured by chemiluminescent detection on a NO_x analyzer (model T200 Teledyne Advanced Pollution Instrument) following reduction to nitric oxide (NO) in a heated iodine solution for NO_2^- (Garside 1982), and reduction in a vanadium (III) solution for NO_3^- plus NO_2^- (Braman 1989).

2.2 N and O Isotope analysis --- NO_3^- $\delta^{15}N$ and $\delta^{18}O$ measurements were made with the denitrifier method (Sigman et al. 2001; Casciotti et al. 2002; McIlvin and Casciotti 2011), wherein denitrifying bacteria lacking terminal nitrous oxide reductase (*P. aureofaciens* ATCC 1398) quantitatively convert NO_3^- and NO_2^- in aqueous samples into N_2O gas. Working cultures grown 7-10 days are concentrated 10-fold by centrifugation and then split into 3-mL aliquots in 20 mL headspace vials. Each vial is crimp sealed and purged for at least 5 hours with N_2 or He. Samples of NO_3^- are injected into the purged vials to obtain 5, 10, or 20 nmoles using a gas tight syringe. Vials are then incubated in the dark overnight to allow for complete conversion of NO_3^- to N_2O. The following day, vials are either frozen for later analysis or extracted, purified, and analyzed on a modified Thermo-Scientific Gas Bench II and Delta V Advantage gas

chromatograph isotope ratio mass spectrometer (IRMS). Samples containing less NO_2^- than corresponding NO_3^- were treated with sulfamic acid to remove NO_2^- and then brought back up to a neutral pH with sodium hydroxide prior to bacterial reduction to N_2O (Granger and Sigman 2009). For samples where NO_2^- concentrations exceeded NO_3^-, NO_2^- was removed via reduction to NO gas by an addition of 1M ascorbic acid and then continuously purged with He for at least 5 hours (Granger et al. 2006). All samples were measured in duplicate against two standards of known isotope composition, IAEA-N3 and USGS-34, which have $\delta^{15}N$ and $\delta^{18}O$ of 4.7‰ and 25.6‰, and -1.8‰ and -27.9‰, respectively (Gonfiantini et al. 1995; Böhlke et al. 2003). Volume of samples was matched by volume of standards to minimize matrix effects on NO_3^- $\delta^{18}O$ (Weigand et al. 2016).

NO_2^- $\delta^{15}N$ and $\delta^{18}O$ isotope analyses with the azide method (McIlvin and Altabet 2005), wherein NO_2^- is completely reduced to N_2O by a 1M sodium azide in a 1.7M acetic acid solution. Samples were diluted in Milli-Q water to 2 mL of 5 μM NO_2^- in 20 mL headspace vials, equivalent to 10 nmoles of NO_2^- in each vial. 2mL of sample, with no dilution, were used when NO_2^- concentrations were lower than 5 μM. All sample vials were flushed with He for 5 minutes, followed by a 15-minute flushing of the sodium azide, acetic acid solution. After flushing, 67 μL of the azide solution was injected into each sample vial using a gas tight syringe and shaken. Samples sat for 30 minutes to allow for complete conversion of NO_2^- to N_2O, after which 67 μL of 6M sodium hydroxide were added to terminate the reaction. NO_2^- isotope analyses for Experiment 2 were performed following a slight modification in which the sodium azide, acetic acid solution was buffered with 0.3 M sodium acetate to ensure that samples and standards reacted at the same pH, which affects oxygen atom equilibration. N_2O isotope ratios were then

analyzed on the IRMS, as described above. Samples were analyzed in duplicate in each of 2-3 respective batch analyses against a combination of six standards of known isotopic values, WILIS 10, WILIS 11, and WILIS 20, which have $\delta^{15}N$ and $\delta^{18}O$ of -1.7‰ and 13.2‰, 57.1‰ and 8.6‰, and -7.8‰ and 47‰, respectively (Scott Wankel, personal communication); and N-23, N-7373, N-12019, which have $\delta^{15}N$ and $\delta^{18}O$ values of 3.7‰ and 11.4‰, -79.6‰ and 4.5‰, and 2.8‰ and 88.5‰, respectively (Böhlke et al. 2007). Oxygen isotope exchange during the azide reaction was corrected for in Experiment 2 samples by diluting select standards and samples in $\delta^{18}O_{H2O}$-enriched water (41.6 ‰) to match those of some samples.

2.3 Regression Analysis --- Type II regressions were conducted in Matlab (Mathworks; Edward Pelter, MBARI) following the method of York et al (1966, 2004), which account for errors in both the X and Y coordinates, in order to derive the slopes and intercepts of $\delta^{18}O_{NO2}$ vs. $\delta^{18}O_{H2O}$ data and $\delta^{18}O_{NO3,produced}$ vs. $\delta^{18}O_{H2O}$ data, and ultimately, isotope effect and exchange terms (see discussion section).

3. Results

3.1 Time-depended evolution of DIN---

3.1.1. The water collected for **Experiment 1** posted NO_3^- and NH_4^+ concentrations of 35 μM and 8 μM, respectively, such that initial NH_4^+ concentrations in experimental incubations were ~58 μM following NH_4^+ additions on day 1 (Fig.3A). Initial NO_2^- concentrations were on the order of 0.2 μM. In all experimental bottles, concentrations of NH_4^+ increased by 0-9 μM over the first week, suggesting ammonification of dissolved organic nitrogen (DON). Despite potential

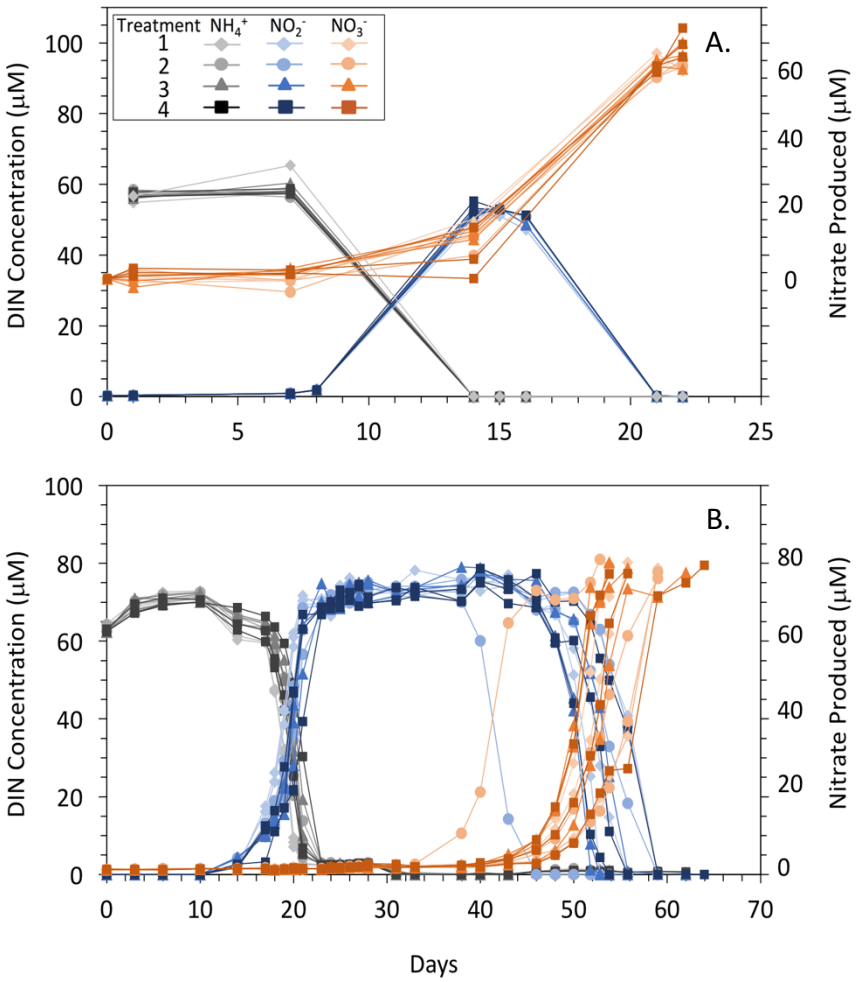

Figure 3*. Time course of NH_4^+, NO_2^-, and NO_3^- concentrations for all incubations following NH_4Cl addition in (A) Experiment 1 and (B) Experiment 2.*

ammonification, NH_4^+ was completely oxidized to NO_2^- by day 14 in all experimental bottles, at which point accumulated NO_2^- was on the order of 50 –53 µM. NO_2^- oxidation to NO_3^- occurred concurrently, the onset of which is unclear given coarse time resolution. Accumulated NO_3^- ranged between 0–17 µM by day 14 (corresponding to 33–50 µM total NO_3^-). NO_2^- was completely oxidized to NO_3^- by day 21, at which point NO_3^- concentrations were on the order of 96-100 µM among treatments, such that ~59-65 µM NO_3^- was produced throughout the incubation – on par with initial [NH_4^+]. Although some NH_4^+ production from the ammonification of DON may have occurred following the onset of NH_4^+ oxidation, DIN species showed apparent mass balance at all sampling points, and NH_4^+ was recovered quantitatively as NO_3^- by the end of the experiment (Fig. 3A) – suggesting that ammonification was only substantive at the onset of the experiment.

3.1.2. The stream water collected for **Experiment 2** had lower initial concentrations of NO_3^- and NH_4^+, of 1.4 μM and 4.8 μM, respectively, and no detectable NO_2^-. Following NH_4^+ addition, initial experimental concentrations were thus ~62 μM (Fig. 3B). As with Experiment 1, [NH_4^+] increased by 7-10 μM in all bottles over the first ten days of incubation, suggesting ammonification of DON. NH_4^+ concentrations remained thus elevated until day 10, after which NH_4^+ concentrations decreased to a minimum of ~2.5 μM by day 23. NH_4^+ concentrations subsequently remained at ~2.5 μM for 10 days before decreasing to below detection on day 33. NO_2^- production was first detected on day 14, accumulating rapidly to 67-75 μM by day 23, then appeared to increase modestly to concentrations of 72-78 μM among treatments by day 33, although this apparent increase is within the uncertainty of the NO_2^- concentration measurements. Nevertheless, among most experimental bottles, peak [NO_2^-] at day 33 exceeded peak [NH_4^+] by an average of 2.1 μM, suggesting that ammonification of DON may have occurred concurrently with NH_4^+ oxidation. NO_3^- production was first detected on day 38 in a single experimental bottle from treatment 2 that reached 75 μM NO_3^- by day 46. Among other experimental bottles, NO_3^- production began in and around day 43, reaching respective maxima at 71-80 μM NO_3^- between days 53 and 64. Final produced NO_3^- concentrations ranged between 70 μM and 79 μM, thus ~14 μM in excess of initial NH_4^+, consistent with the ammonification of DON.

3.2 Evolution of $\delta^{18}O$ and $\delta^{15}N$ of NO_2^- and NO_3^- ---

3.2.1. Experiment 1

3.2.1(a) *$\delta^{18}O$ of NO_2 and NO_3^- in Experiment 1*--- The $\delta^{18}O_{NO2}$ in Experiment 1 was first measured on day 8, when $[NO_2^-]$ was ~1.9 μM among treatments, corresponding to an f_{NO2} value of 4% - where f_{NO2} is the fraction of the $[NO_2^-]$ measured relative the maximum $[NO_2^-]$ observed in each incubation, $[NO_2^-]/[NO_{2\,max}^-]$ (Fig. 4A). This metric rests on the premise that $[NO_{2\,max}^-]$ reflects the sum product of NH_4^+ oxidation, not yet diminished by NO_2^- oxidation to NO_3^-, an assumption that is not entirely accurate given that up to 10 μM NO_3^- was already produced at peak NO_2^-. Nevertheless, $\delta^{18}O_{NO2}$ values first measured on day 8 were -0.7 ± 0.3‰, -1.3 ± 0.4‰, 1.6 ± 0.2‰, and 6.7 ± 0.6‰ for treatments 1-4, respectively, increasing to values of 5.9 ± 0.5‰, 5.3 ± 0.3‰, 6.2 ± 0.2‰, and 6.8 ± 0.3‰ just after peak $[NO_2^-]$ on day 15 (f_{NO2} = 1). Given coarse time resolution, we take these values to correspond roughly to the "final" $\delta^{18}O_{NO2}$ produced from NH_4^+ oxidation prior to the onset of NO_2^- oxidation. These final $\delta^{18}O_{NO2}$ values were distinctly lower than expected from the weighted source attribution model of Eq. 1, by ~4‰ for treatments 1 and 2 and ~2‰ for treatments 3 and 4 (Fig. 4A). Following peak $[NO_2^-]$, $\delta^{18}O_{NO2}$ values then decreased by 0-1.5‰ by day 16 as NO_3^- accumulated (f_{NO2} ~ 0.92). At the subsequent sampling on day 21, remaining NO_2^- concentrations were too deplete to measure $\delta^{18}O_{NO2}$ (~0.2 μM).

The initial $\delta^{18}O_{NO3}$ in the stream water was 4.1 ± 0.2‰ (f_{NO3} ~ 0; where $f_{NO3} = [NO_3^-]/[NO_{3\,max}^-]$) (Fig. 4B). By the first sampling of accumulated NO_3^- on day 14, $[NO_3^-]$ had increased by ~15 μM (f_{NO3} ~ 0.25) among treatments, although cumulative $\delta^{18}O_{NO3,total}$ values remained close to initial values at ~4‰. As $[NO_3^-]$ increased further, $\delta^{18}O_{NO3}$ values then decreased, resulting in respective final $\delta^{18}O_{NO3,total}$ (f_{NO3} = 1.0) of -2.3 ± 0.1‰, -2.2 ± 0.1‰, -1.6 ± 0.1‰, and -0.8 ± 0.1‰, for treatments 1 through 4.

Values of $\delta^{18}O_{NO3}$ corresponding to the NO_3^- specifically produced during the experiments ($\delta^{18}O_{NO3,produced}$), derived from the weighted difference from total NO_3^-, ranged from 0.91 ± 0.5‰ to 4.3 ± 1.6‰ among treatments on day 14 ($0.07 < f_{NO3} < 0.28$; Fig. 4C). As $[NO_3^-]$ increased further, the $\delta^{18}O_{NO3,produced}$ decreased to cumulative final values of -5.8 ± 0.2‰, -5.7 ± 0.2‰, -4.7 ± 0.3 ‰, and -3.4 ± 0.3 ‰ for treatments 1 through 4, respectively, in apparent proportion to corresponding $\delta^{18}O_{H2O}$ treatments. As with $\delta^{18}O_{NO2}$, however, values of $\delta^{18}O_{NO3,produced}$ at the final sampling were substantially lower than expected from fractional source attribution of O atoms (Eq. 2) by 9.3‰, 9.4‰, 9.1‰, and 8.7‰ for respective $\delta^{18}O_{H2O}$ treatments (Fig. 4C).

3.2.1(b) $\delta^{15}N$ of NO_2 and NO_3^- in Experiment 1 --- The corresponding $\delta^{15}N_{NO2}$ followed a unified trend among treatments in Experiment 1, with values of -25.0 ± 0.9‰ on day 8, increasing by 34‰ to a maximum of 8.9 ± 0.2‰ on day 15 (f_{NO2} = 1.0), (Fig 4D). As with $\delta^{18}O_{NO2}$, $\delta^{15}N_{NO2}$ values then decreased following peak $[NO_2^-]$, by ~1‰ in all treatments by day 17 (f_{NO2} = 0.92). Concurrently, values of $\delta^{15}N_{NO3,total}$ deceased slightly over the course of the experiment among all treatments (Fig. 4E); Initial values in stream water were 8.2 ± 0.1‰ (f_{NO3} = 0), compared to 7.7 ± 0.1‰ (f_{NO3} = 1.0) at the final sampling. Derived values for the NO_3^- produced cumulatively, $\delta^{15}N_{NO3,\ produced}$, ranged from 7.6 ± 0.5‰ to 9.5 ± 0.5‰ on day 14 ($0.07 < f_{NO3} < 0.28$), then decreased to a cumulative final value of 7.4 ± 0.2‰ (f_{NO3} = 1.0) among all treatments (Fig. 4F). The limited change in $\delta^{15}N_{NO3,\ total}$ throughout the course of the experiment is thus explained by a $\delta^{15}N$ of initial NH_4^+ pool (~6.8‰) that was similar to that of initial NO_3^- $\delta^{15}N$ (8.2‰) in the incubations.

3.2.2. Experiment 2

3.2.2(a) $\delta^{18}O$ of NO_2^- and NO_3^- Experiment 2--- $\delta^{18}O_{NO2}$ in Experiment 2 was first measured on day 17, when 10-17 μM NO_2^- had accumulated among experimental bottles (f_{NO2} ~ 0.15; Fig.4G) posting values of -6.2 ± 0.2‰, -3.2 ± 0.4‰, 5.2 ± 0.4‰, and 18.9 ± 0.5‰ in treatments 1-4, respectively. Values in all incubations then increased by ~8‰ as [NO_2^-] increased concurrently by less than 10 μM, $\delta^{18}O_{NO2}$ values increased by 2.5‰, 4.3‰, 5.5‰, and 8.9‰ in respective treatments 1-4, resulting in $\delta^{18}O_{NO2}$ at [NO_2^-] maxima of 3.9 ± 0.4‰, 9.2 ± 0.2‰, 17.8 ± 0.7‰, and 34.4 ± 0.9‰. We consider these latter values to be the final $\delta^{18}O_{NO2}$ produced from NH_4^+ oxidation. These are notably lower than predicted based on fractional source attribution for O atoms (Eq. 1) for treatments 1, 2, and 3 by 7.1‰, 4.8‰, and 2.0‰ respectively, whereas they are greater than predicted for treatment 4 by 5.2‰. Following the onset of NO_3^- production, $\delta^{18}O_{NO2}$ continued to increase slightly to maximum values of 5.1 ± 0.4‰, 10.3 ± 0.1‰, 19.5 ± 0.3‰, and 36.5 ± 0.4‰. After approximately half of the NO_2^- had been oxidized to NO_3^- the $\delta^{18}O_{NO2}$ began to decrease, resulting final measurements of $\delta^{18}O_{NO2}$ that were 3-7‰ lower than respective maxima.

$\delta^{18}O_{NO3,total}$ values rapidly increased at the onset of NO_3^- production, from an initial (f_{NO3} = 0.0) $\delta^{18}O_{NO3}$ value of -5.5 ± 0.8‰ in stream water, to 4.1 ± 1.0‰, 7.6 ± 0.3‰, 15.0 ± 0.5‰, and 30.4 ± 0.7‰ ($0.05 < f_{NO3} < 0.15$) in respective treatments 1-4 (Fig. 4H), reflecting mixing of newly produced NO_3^- with the modest ambient pool of stream water NO_3^- (of 1.4 μM). $\delta^{18}O_{NO3,total}$ values then evolved gradually as NO_2^- oxidation proceeded, posting final (f_{NO3} = 1.0)

$\delta^{18}O_{NO3,total}$ values of 0.1 ± 0.1‰, 5.1 ± 0.3‰, 14.7± 0.7‰, and 32.9 ± 0.4‰. The corresponding $\delta^{18}O_{NO3,produced}$ produced at the onset of NO_2^- oxidation ($0.05 < f_{NO3} < 0.19$) were 3.8 ± 0.7‰, 11.4± 0.6‰, 18.6 ± 0.7‰, and 37.7 ± 0.7‰, for treatments 1-4, respectively (Fig. 4I), gradually decreasing among treatments to final values ($f_{NO3} = 1$) of 0.0 ± 0.1‰, 5.3 ± 0.2‰, 15.1 ± 0.8‰, and 33.6 ± 0.4‰. As such, the final $\delta^{18}O_{NO3,produced}$ values were lower than would be predicted by Eq. 2 for treatments 1-3 by 6.6‰, 5.3‰, and 2.0‰, respectively, and higher than predicted by 3.2‰ for treatment 4.

3.2.2(b) $\delta^{15}N$ of NO_2^- and NO_3^- Experiment 2--- The $\delta^{15}N$ of the NO_2^- produced initially ($0.05 < f_{NO2} < 0.11$; Fig. 4J) was -18.6 ± 0.4‰, averaged among treatments, and increased by ~29‰ to a maximum value 9.8 ± 0.2‰ at peak NO_2^- concentrations ($f_{NO2} = 1.0$). As NO_2^- was depleted, $\delta^{15}N_{NO2}$ decreased to ~ -6.0‰ ($f_{NO2} \sim 0.10$). The stream water NO_3^- had an initial $\delta^{15}N_{NO3}$ value of 10.8 ± 0.2‰. In a similar trend to $\delta^{18}O_{NO3,total}$, $\delta^{15}N_{NO3,total}$ values rapidly increased at the onset of NO_2^- oxidation, rising to an average value of 16.2 ± 0.9‰ ($f \sim 0.10$) among treatments, before gradually decreasing to a final value of 7.8 ± 0.1‰ (Fig. 4K). The $\delta^{15}N_{NO3,produced}$ values at the onset of NO_3^- production ($f_{NO3} < 0.10$) ranged from 15.8 ± 0.4‰ to 20.0 ± 0.6‰ (Fig. 4L). The $\delta^{15}N_{NO3,produced}$ decreased gradually as NO_3^- was produced, to a cumulative final $\delta^{15}N_{NO3,produced}$ ($f = 1$) of 7.7 ± 0.1‰ among treatments.

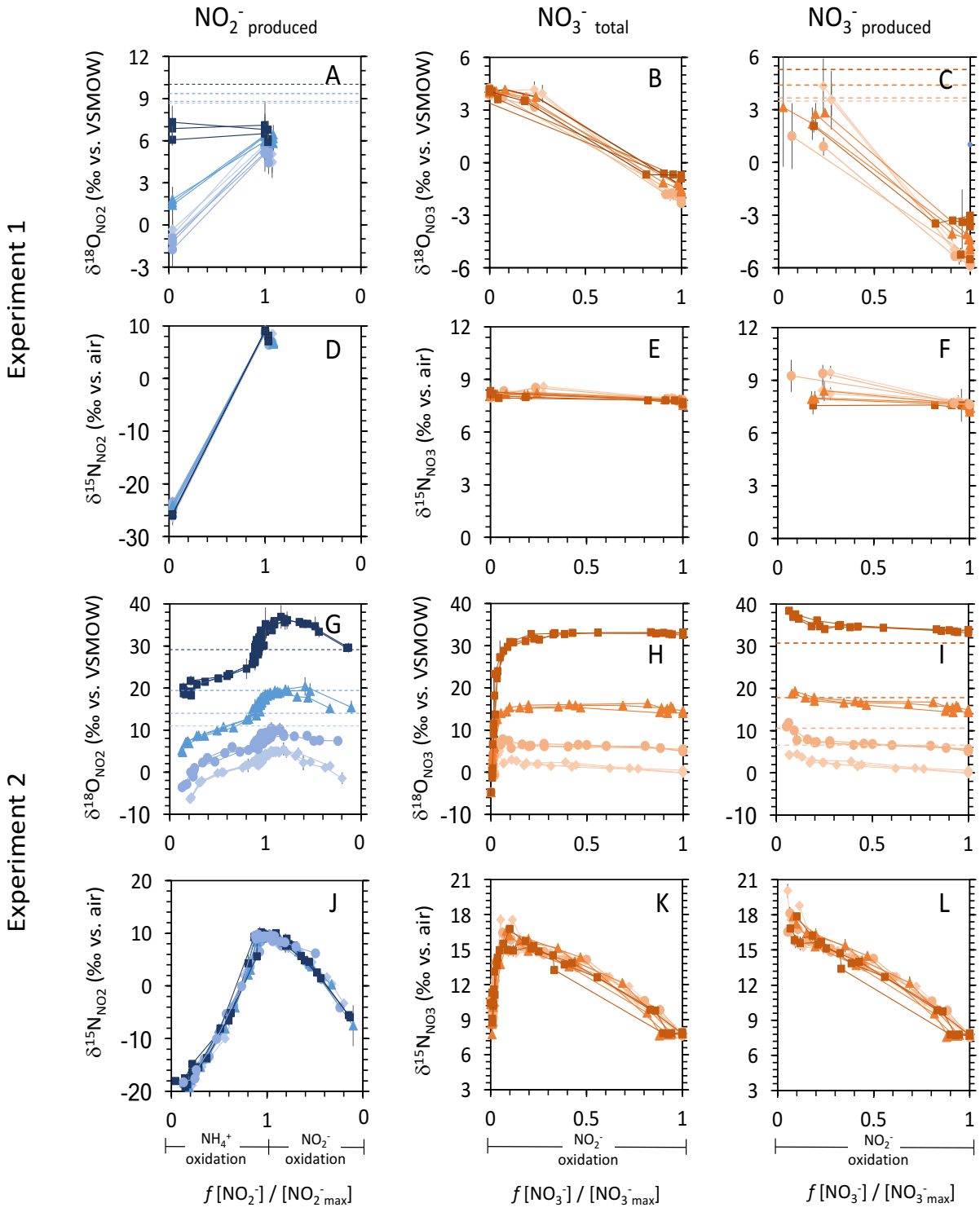

Figure 4. Concentration-dependent evolution of $\delta^{18}O_{NO2}$ (A), $\delta^{15}O_{NO3\ total}$ (B), $\delta^{18}O_{NO3\ produced}$ (C), $\delta^{15}N_{NO2}$ (D), $\delta^{15}N_{NO3\ total}$ (E), and $\delta^{15}N_{NO3,produced}$ (F) during Experiment 1; and $\delta^{18}O_{NO2}$ (G), $\delta^{18}O_{NO3\ total}$ (H), $\delta^{18}O_{NO3\ produced}$ (I), $\delta^{15}N_{NO2}$ (J), $\delta^{15}N_{NO3\ total}$ (K), and $\delta^{15}N_{NO3,produced}$ (L) during Experiment 2. The x-axis, f_{NOx}, *corresponds to the fraction of NO_x at the time of sampling relative to the maximum concentration of NO_x observed over the entire experiment. The color and marker scheme is the same as in Fig. 3, with NO_2^- presented in shades of blue and NO_3^- presented in shades of orange, and where shading (light to dark) corresponds to respective treatments (1-4). In addition, diamond markers correspond to treatment 1, circle markers correspond to treatment 2, triangle markers correspond to treatment 3, and square markers correspond to treatment 4. Dashed, colored lines correspond to the expected $\delta^{18}O$ of NO_2^- (panels A and G) and NO_3^- (panels C and I) for each $\delta^{18}O_{H2O}$ treatment according to Eq. 1 and 2. Error bars are analytical error for all panels with the exception of $\delta^{18}O$ and $\delta^{15}N$ of $NO_3^-{}_{produced}$ (C, F, I, and L), in which case the errors are derived from propagation of analytical uncertainty on $\delta^{18}O$ and $\delta^{15}N$ of NO_3^-.*

3.3 Dependence of $\delta^{18}O_{NO2}$ and $\delta^{18}O_{NO3}$ on $\delta^{18}O_{H2O}$--- The values of $\delta^{18}O_{NO2}$ at peak NO_2^- displayed a linear dependence on $\delta^{18}O_{H2O}$ in both experiments (Fig 5A and 5B). Respective slopes of fitted linear regressions for both experiments are 0.63 ± 0.14 and 0.73 ± 0.003 respectively, greater than the value of 0.50 otherwise expected from Eq. 1, thus signaling a greater dependence of $\delta^{18}O_{NO2}$ on the $\delta^{18}O$ of H_2O. The respective intercepts, 9.5 ± 0.8 and 5.2 ± 0.0, are lower than the value of 12.1 (one half of $\delta^{18}O_{O2}$) expected from Eq. 1, assuming a

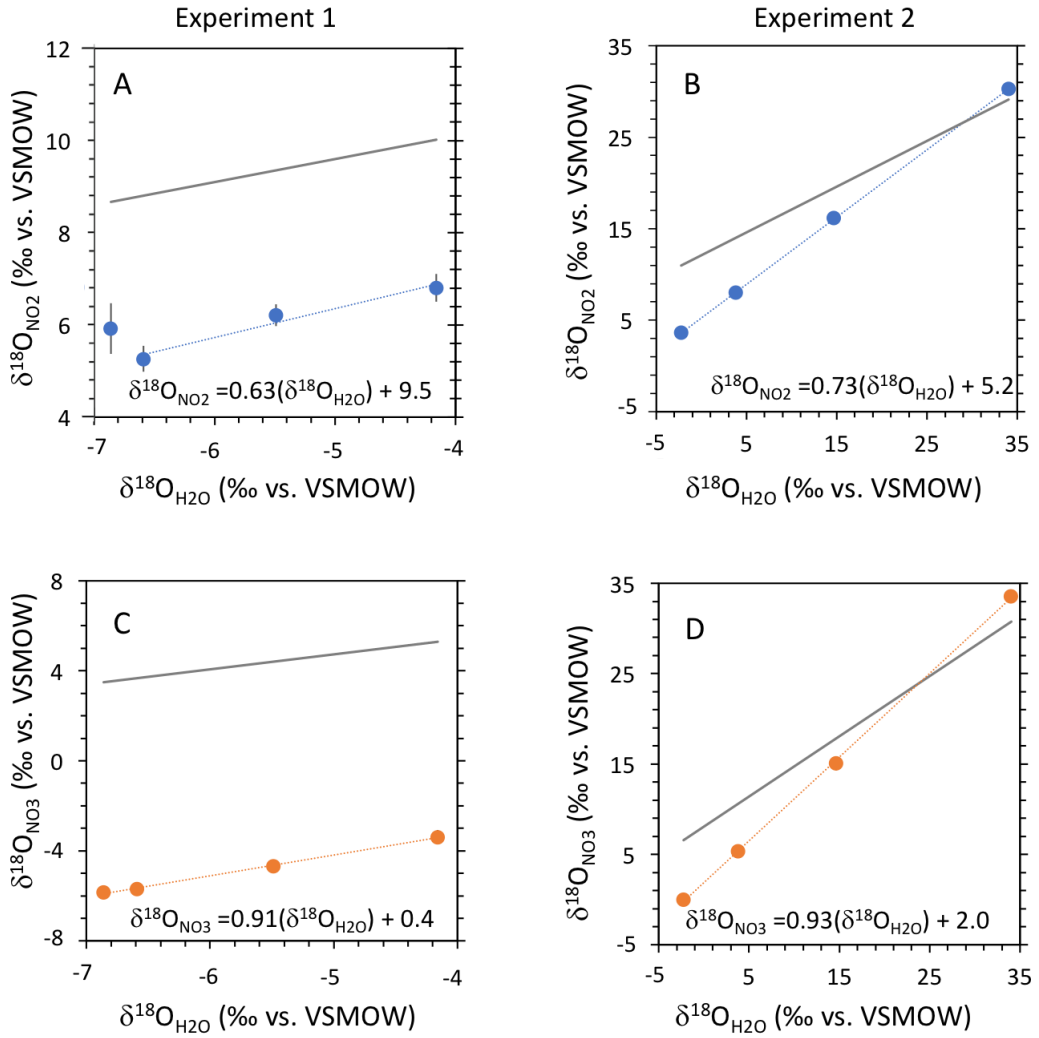

Figure 5. Intermediate $\delta^{18}O_{NO2}$ vs. $\delta^{18}O_{H2O}$ for Exp. 1 (A) and Exp. 2 (B) and final $\delta^{18}O_{NO3,\ produced}$ vs. $\delta^{18}O_{H2O}$ for Exp. 1 (C) and Exp. 2 (D). Dashed lines and equations are linear regressions fit to the data using Matlab. $\delta^{18}O_{NO2}$ and $\delta^{18}O_{NO3}$ expected from Eq. 1 and 2 are represented in each plot in grey. Error bars are the standard deviation of triplicate bottle measurements.

$\delta^{18}O_{O2}$ of 24.2‰ for air-equilibrated O_2 (Kroopnick & Craig, 1972). We note that given the very slow growth rates of nitrifiers in our incubations as well as agitation during sampling, $\delta^{18}O$ of O_2 was likely close to equilibrium value throughout the experiments.

Similarly, $\delta^{18}O$ of final produced NO_3^- also show linear dependence, with slopes of 0.91 ± 0.04 and 0.93 ± 0.01 and intercepts of 0.4 ± 0.3 and 2.0 ± 0.1 (Fig 5C and 5D). As with $\delta^{18}O_{NO2}$, the regression slopes are greater than the expected 0.66 and the intercepts lower than the 8.1 expected from the fractional source contribution model, Eq. 2.

4. Discussion

The oxygen isotope composition of NO_2^- and NO_3^- produced from the oxidation of NH_4^+ showed a direct dependence on $\delta^{18}O_{H2O}$ among treatments, albeit, in proportions different than expected from simple fractional contributions of O atom sources. The divergence from direct source attribution suggests the influence of kinetic isotope effects on O during incorporation, as well as O atom equilibration of NO_2^- with H_2O and associated equilibrium isotope effects, as documented in cultures of nitrifying prokaryotes (Buchwald & Casciotti, 2010; Buchwald et al., 2012; Casciotti et al., 2010; Snider et al., 2010). Below, we first examine the evolution of NO_2^- O isotopes to discern the potential influence of isotope effects and O atom equilibration during its production (NH_4^+ oxidation) and during its consumption (NO_2^- oxidation). We then assess the concurrent evolution of NO_3^- isotopes to confirm inferences gleaned from NO_2^- isotope measurements. Based on the dynamics uncovered, we discuss implications for detecting nitrification in the environment from NO_3^- $\delta^{18}O$, and for the interpretation of NO_3^- isotope distributions in freshwater environments.

4.1 $\delta^{18}O$ of NH_4^+ oxidation ---

On the basis that the O atoms incorporated during the oxidation of NH_4^+ to NO_2^- derive from molecular O_2 and H_2O (Andersson & Hooper, 1983), then the $\delta^{18}O$ of NO_2^- produced by nitrification in our experiments would correspond to the weighted sum of the $\delta^{18}O$ of end members (Eq. 1), barring the influence of incorporation isotope effects. The $\delta^{18}O$ of NO_2^- thus produced would also remain invariant throughout the time course of the experiments – as the $\delta^{18}O$ of the O_2 and H_2O substrate pools remain constant – unless NO_2^- was subject to progressive O-atom equilibration with H_2O. Contrary to these expectations, however, the $\delta^{18}O$ of NO_2^- produced at the onset of NH_4^+ oxidation in both experiments was substantially lower than predicted by the weighted sum (Eq. 1; Fig. 4A and 4G). The low $\delta^{18}O$ of NO_2^- values initially produced suggest isotopic discrimination during O-atom incorporation from either O_2, H_2O, or both. As NH_4^+ oxidation proceeded, the $\delta^{18}O$ of NO_2^- increased to respective $\delta^{18}O$ maxima at peak $[NO_2^-]$ in all but one treatment, which had the highest experimental $\delta^{18}O_{H2O}$ (Experiment 2), in which $\delta^{18}O_{NO2}$ decreased. This $\delta^{18}O_{NO2}$ change among treatments is consistent with NO_2^- equilibration with H_2O and associated isotope effect, where $\delta^{18}O_{NO2}$ equilibrates to a value on the order of $\delta^{18}O_{H2O}$ + 13‰ at room temperature (Buchwald & Casciotti, 2013; Casciotti et al., 2007). At peak NO_2^- concentrations in both experiments, the $\delta^{18}O_{NO2}$ was lower than expected for full equilibration among treatments, suggesting partial equilibration.

The observations may thus show better correspondence to a more comprehensive model of NH_4^+ oxidation that considers incorporation isotope effects on oxygen atoms of molecular O_2 and H_2O, as well as fractional oxygen atom equilibration of NO_2^- with H_2O with a corresponding equilibrium isotope effect (Eq. 3; Casciotti et al., 2010; Buchwald et. al, 2012).

Where $X_{NO2,1}$ is the fraction of NO_2^- oxygen atoms that have equilibrated with H_2O, $^{18}\varepsilon_{k,O2}$ is the kinetic isotope effect for O_2 incorporation, $^{18}\varepsilon_{k,H2O,1}$ is the kinetic isotope effect for H_2O incorporation, and $^{18}\varepsilon_{eq}$ is the equilibrium isotope effect for NO_2^- equilibration with water (Casciotti et al. 2010).

$$\delta^{18}O_{NO2} = [\tfrac{1}{2}(\delta^{18}O_{O2} - {}^{18}\varepsilon_{k,O2}) + \tfrac{1}{2}(\delta^{18}O_{H2O} - {}^{18}\varepsilon_{k,H2O,1})](1 - X_{NO2,1}) + (\delta^{18}O_{H2O} + {}^{18}\varepsilon_{eq})(X_{NO2,1}) \quad (3)$$

Equation 3 can be re-arranged to a linear model describing $\delta^{18}O_{NO2}$ vs. $\delta^{18}O_{H2O}$ (Fig. 7A and B).

$$\delta^{18}O_{NO2} = (\tfrac{1}{2} + \tfrac{1}{2}X_{NO2,1})\delta^{18}O_{H2O} + \tfrac{1}{2}[(\delta^{18}O_{O2} - {}^{18}\varepsilon_{k,O2} - {}^{18}\varepsilon_{k,H2O,1})(1\text{-}X_{NO2,1})] + (X_{NO2,1}{}^{18}\varepsilon_{eq}) \quad (4)$$

From Eq. 4 and the linear regression of peak NO_2^- $\delta^{18}O_{NO2}$ (Fig. 5A and 5B), we can estimate the fraction of NO_2^- O atoms that had exchanged with H_2O by the time of sampling ($X_{NO2,1}$) from the regression slope and the combined O incorporation isotope effect ($^{18}\varepsilon_{k,\,O2}$ + $^{18}\varepsilon_{k,\,H2O,1}$) during NH_4^+ oxidation from the regression intercept. We assume that O_2 in our experimental bottles was in equilibrium with air, $\delta^{18}O_{O2}$ of 24.2‰ (Kroopnick & Craig, 1972), and an NO_2^-–H_2O equilibrium isotope effect ($^{18}\varepsilon_{eq}$) of 13‰ for both abiotic and biologically mediated exchange (Buchwald & Casciotti, 2013; Karen L. Casciotti et al., 2007). From the slope of the $\delta^{18}O_{NO2}$ regression (Fig. 5A and 5B) we derive $X_{NO2,1}$ values of 26 ± 27% for Experiment 1 and 47 ± 1 % for Experiment 2. The sizeable uncertainty in the estimates for Experiment 1 derives from the poor sampling resolution, and may also reflect that some fraction of NO_2^- was already oxidized to NO_3^- at peak [NO_2^-]. Nevertheless, the proportion of NO_2^- O atom

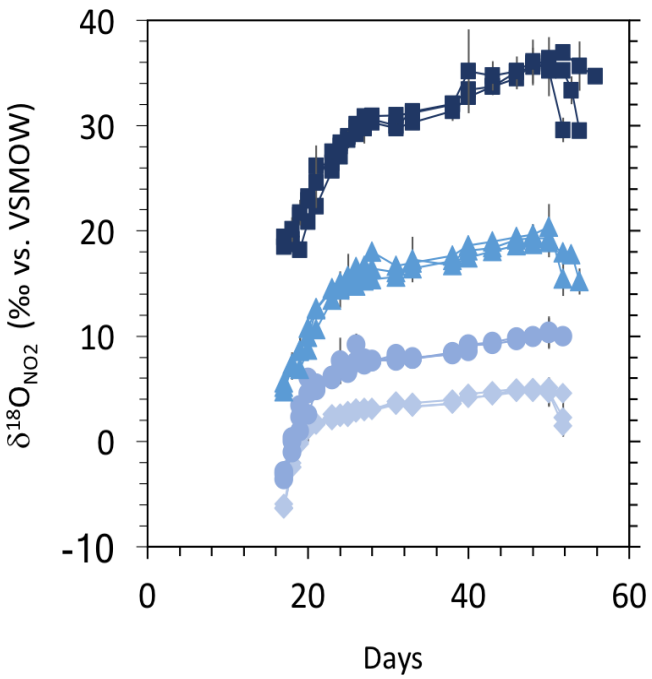

Figure 6. Time dependent evolution of $\delta^{18}O$ NO_2^- produced among treatments and bottle triplicates in Experiment 2. Error bars are standard deviations of analytical replicates.

equilibrated with H_2O computed here are comparable to values observed in a NH_4^+ oxidizing cultures (Casciotti et al., 2010; Table 2).

We note that our equilibration estimates here conflate both abiotic and biologically-mediated equilibration, contrasting estimates from cultures in Table 2 which represent fraction of biologically-mediated exchange exclusively. O atom equilibration between NO_2^- and H_2O occurs inorganically, as a function of pH, temperature, and NO_2^- residence time, but can also be facilitated by some NH_4^+ oxidizing bacteria and archaea (Casciotti et al., 2010). Inorganic equilibration is expectedly slow at the pH of our incubations, on order of 10 - 30% over 3 weeks (Casciotti et al., 2007).

While we cannot readily distinguish between abiotic and biologically mediated exchange in our incubations, we observed a relatively rapid increase in $^{18}O_{NO2}$ during the first 3-9 days of active NH_4^+ oxidation in Experiment 2 (Fig. 6), which we interpret as dominated by biotically-mediated exchange during active NH_4^+ oxidation. Near the end of the steep increase in $\delta^{18}O_{NO2}$, on day 23, the fraction of NO_2^- isotopically equilibrated with water was ~ 27%, in the upper range of biologically mediated exchange observed for NH_4^+ oxidizing cultures (Casciotti et al., 2010; Table 2). Equilibration was subsequently slower during the following two weeks where

Table 2. Isotope effects and fraction of NO_2^- isotopically equilibrated with H_2O (X_{NO2}) in our experiments, compared to existing estimates from nitrifier culture studies and sea water incubations ([1]Buchwald et al., 2012; [2]Casciotti et al., 2010; [3]Casciotti et al., 2003; [4]Marrioti et al., 1981; [5]Buchwald and Casciotti, 2010). X_{NO2} values from culture experiments correspond to biologically mediated equilibration only, whereas X_{NO2} values from our experiments and seawater incubations conflate abiotic and biologically mediated equilibration. ‡Kinetic isotope effect does not factor out competing contribution of coincident O-atom equilibration with NO_2^-.

	Exp. 1 (n = 1)	Exp. 2 (n = 1)	Seawater Incubations (n = 7)[1]	Co-cultures (n = 6)[1]	NH_4^+ oxidizing cultures (n = 10)[2,3,4]	NO_2^- oxidizing cultures (n = 3)[5]
$X_{NO2,1}$ (%)	26 ± 27	47 ± 1	35 – 100	16 – 28	1 – 25	ND
$X_{NO2,2}$ (%)	74 ± 12	78 ± 3	48 – 100	0 -26	ND	0 – 3
$^{18}\varepsilon_{k,H2O,1}+^{18}\varepsilon_{k,O2}$ (‰)	7.6 ± 17.8	27.5 ± 4.0	11 – 20	16 – 23	18 – 30	ND
$^{18}\varepsilon_{k,H2O,2}$ (‰)	22.5 ± 6.5	13.5 ± 2.0	1 – 27	6 – 12	ND	9 – 25
$^{18}\varepsilon_{k,NO2}$ (‰)	ND	-3.9 ± 0.3‡	ND	ND	ND	-10 – -1.4
$^{15}\varepsilon_{k,AMO}$ (‰)	ND	34.5 ± 0.2	ND	ND	14 – 38	ND
$^{15}\varepsilon_{k,NO2}$ (‰)	ND	-10.3 ± 0.4 -8.7 ± 0.2	ND	ND	ND	-21 – -9

ambient NO_2^- remained elevated (≥70 μM; Fig. 6), reaching 45% prior to the onset of NO_3^- production. The extent to which this slower equilibration was abiotic or biotically catalyzed is uncertain. Equlibration on the accumulated NO_2^- pool presumalbly continued during subsequent NO_3^- production, although apparent inverse isotopic discrimination of NO_2^- O atoms at the onset of NO_3^- production obfuscates any visual trend of equilibration in the $\delta^{18}O_{NO2}$ data (Fig. 6).

From the intercepts of the $\delta^{18}O_{NO2}$ vs. $\delta^{18}O_{H2O}$ regressions (Fig. 5A and 5B), we derive combined O atom incorporation isotope effects, $^{18}\varepsilon_{k,\,O2} + {}^{18}\varepsilon_{k,\,H2O,1}$, of 7.6 ± 17.8‰ and 27.5 ± 4.0‰ for Experiments 1 and 2 respectively (Eq. 6). As mentioned in the Results, some NO_2^- had already been consumed at the sampling for intermediate NO_2^- used in Fig. 5A, rendering uncertain the estimate of the combined isotope effect for Experiment 1. Nevertheless, values for both experiments are within the observed range of culture and seawater incubation studies

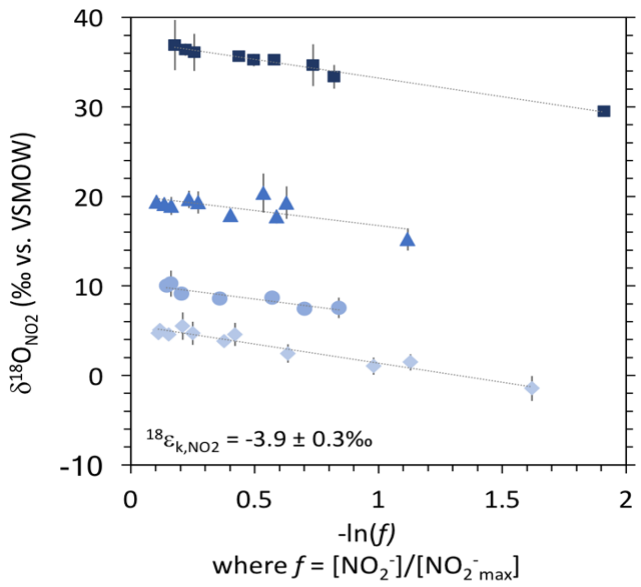

Figure 7. $\delta^{18}O_{NO2}$ vs $ln(f_{NO2})$ during NO_2^- oxidation among $\delta^{18}O_{H2O}$ treatments (Experiment 2). Progressive darker shades of blue correspond to incremental $\delta^{18}O_{H2O}$ treatment. Blue diamond markers correspond to treatment 1 and square markers correspond to treatment 4. Error bars are the standard deviation of triplicate bottle measurements.

(Table 2; Buchwald et al., 2012; Casciotti et al., 2010). In all, the $\delta^{18}O$ of NO_2^- produced from biological NH_4^+ oxidation in stream water incubations was subject to incorporation isotope effects (for either H_2O or O_2 O atom incorporation, or both) and was further dependent on $\delta^{18}O$ of H_2O as a function of NO_2^- equilibration and the associated isotope effect.

4.2 $\delta^{18}O$ of NO_2^- oxidation ---

During biological NO_2^- oxidation, the O atom appended to NO_3^- derives from H_2O (Kumar et al., 1983). To a first approximation, the $\delta^{18}O$ of NO_3^- produced during nitrification should reflect to the weighted sum of the $\delta^{18}O$ end members (Eq. 2), barring the potential influence of (a) an O atom incorporation isotope effect, (b) isotopic exchange of NO_2^- with H_2O, and (c) a kinetic isotope effect on O atoms of NO_2^- during its oxidation to NO_3^-. The $\delta^{18}O$ of NO_3^- thus produced would also remain constant within individual treatments throughout the experiment. Countering the latter expectation, the $\delta^{18}O_{NO3,\ produced}$ at onset of NO_3^- production decreased continually among all treatments in both experiments (Fig. 4C and 4I). This trend is consistent with inverse isotope discrimination on the O atoms during NO_2^- oxidation ($^{18}\varepsilon_{k,NO2}$), which has been documented in culture studies of NO_2^- oxidizing bacteria (Buchwald & Casciotti, 2010; Casciotti, 2009). Inverse isotope fractionation of

O is also apparent in the $\delta^{18}O_{NO2}$ data from the decreasing trend in $\delta^{18}O_{NO2}$ as it is oxidized to NO_3^-. The high temporal resolution in Experiment 2 allows for an estimate of the inverse O isotope effect on NO_2^- from the closed-system Rayleigh product equation (Mariotti et al., 1981):

$$\overline{\delta}_{product} = \delta_{substrate,initial} - \varepsilon \times \frac{f \ln(f)}{(1-f)} \qquad (5)$$

where f is fraction of the substrate (NO_2^-) remaining relative to the initial substrate concentration. The resulting value of $^{18}\varepsilon_{k,NO2}$ is ~ -3.9‰ (Fig. 7), which is comparable to values reported for culture studies (Buchwald and Casciotti, 2010; Table 2). However, we note that this value is uncertain given a potentially competing effect of ongoing NO_2^- equilibration.

In order to determine whether NO_2^- was subject to further O atom equilibration following the onset of NO_3^- production, we investigate the correspondence of NO_3^- O isotope dynamics to the more comprehensive description of NO_2^- oxidation that account for equilibration as well as potential incorporation isotope effects (Eq. 6; Buchwald and Casciotti, 2010; Buchwald et. al, 2012). The potential for equilibration of NO_2^- with H_2O during NO_2^- oxidation is also featured in Eq. 6. However, the biological catalysis of equilibration was found to be negligible during NO_2^- oxidation (Buchwald and Casciotti, 2010). Nevertheless Eq. 6 accounts for pH-dependent inorganic equilibration, which occurs on pertinent time scales and is denoted as X_{NO2} for completeness. We note that as presented, Eq. 6 neglects the inverse kinetic isotope effect for NO_2^- conversion to NO_3^- given complete oxidation of NO_2^- to NO_3^-; it would however be pertinent in the case of incomplete NO_2^- oxidation.

$$\delta^{18}O_{NO3,\,\text{nitrified}} = \frac{2}{3}\left[(1 - X_{NOB})\delta^{18}O_{NO2,initial} + X_{NO2}(\delta^{18}O_{H2O} + {}^{18}\varepsilon_{eq})\right] + \frac{1}{3}(\delta^{18}O_{H2O} - {}^{18}\varepsilon_{k,H2O,2}) \qquad (6)$$

With the substitution of $\delta^{18}O_{NO2}$ terms from Eq. 3, Eq. 6 is rearranged to conform to a linear formulation of $\delta^{18}O_{NO3,\ nitrified}$ vs. $\delta^{18}O_{H2O}$. From the linearized Eq. 7, we estimate the final fraction of NO_2^- O atoms exchanged with H_2O over the entire time course of our experiments ($X_{NO2,2}$) from the slope, and the third O incorporation isotope effect ($^{18}\varepsilon_{k,H2O,2}$) during NO_2^- oxidation from the intercept (Buchwald and Casciotti, 2010; Buchwald et. al, 2012). To solve for $X_{NO2,2}$ and $^{18}\varepsilon_{k,H2O,2}$ in Eq. 7, we assume the same values for $\delta^{18}O_{O2}$ and $^{18}\varepsilon_{eq}$ as for $\delta^{18}O_{NO2}$ analysis and we use the respective $^{18}\varepsilon_{k,\ O2} + {}^{18}\varepsilon_{k,\ H2O,1}$ derived from each experiment.

$$\delta^{18}O_{NO3,\,\text{nitrified}} = \left(\frac{2}{3} + \frac{1}{3}X_{NO2,2}\right)\delta^{18}O_{H2O} + \frac{1}{3}\left[\left(\delta^{18}O_{O2} - {}^{18}\varepsilon_{k,O2} - {}^{18}\varepsilon_{k,H2O,1}\right)(1-X_{NO2,2}) - {}^{18}\varepsilon_{k,H2O,2}\right] + \frac{2}{3}\left(X_{NO2,2}\,{}^{18}\varepsilon_{eq}\right) \quad (7)$$

The total fraction of NO_2^- O-atom equilibration with H_2O was 74 ± 12% and 78 ± 3% in Experiments 1 and 2 respectively. These values are comparable to those observed during incubations of natural seawater assemblages (Buchwald et al., 2012) (Table 2), where high concentrations (upwards of 50 μM) of accumulated NO_2^- remained present for at least 13 days prior to the onset of NO_2^- oxidation. In similar experiments with NH_4^+ oxidizing and NO_2^- oxidizing co-cultures (Buchwald et al., 2012), less than 28% of NO_2^- O atoms had exchanged with H_2O. This difference is presumably due to substantially shorter residence times of NO_2^- in the co-culture experiments, resulting in a decreased potential for abiotic equilibration. Biologically-mediated exchange by NO_2^- oxidizing cultures is thought to be negligible (Buchwald and Casciotti, 2010). Therefore, the increase of fraction of NO_2^- exchanged calculated from

$\delta^{18}O_{NO2}$ data to 74% and 78% (from values of 26% and 47% at the onset of NO_3^- production) may derive dominantly from abiotic equilibration.

From the intercepts of $\delta^{18}O_{NO3,produced}$ vs. $\delta^{18}O_{H2O}$ linear regressions, we derive respective values of 22.5 ± 6.5‰ and 13.5 ± 2.0‰ for the O atom incorporation isotope effect during NO_2^- oxidation in Experiments 1 and 2. These values are on par with those observed in NO_2^- oxidizing monocultures, and incubations of nitrifying co-culture and natural assemblage seawater experiments (Buchwald & Casciotti, 2010; Buchwald et al., 2012). Thus, the NO_2^- oxidation step in stream water incubations is subject to both incorporation and inverse kinetic isotope effects, as well as ongoing NO_2^- equilibration, analogous to cultures and marine incubations (Table 2).

4.3 N isotope dynamics ---

While not the focus of this study, the N isotope dynamics of experimental incubations provide additional support regarding the influence of isotopic discrimination on produced NO_3^-. Initial NO_2^- N was isotopically light and increased during production, which is consistent with a

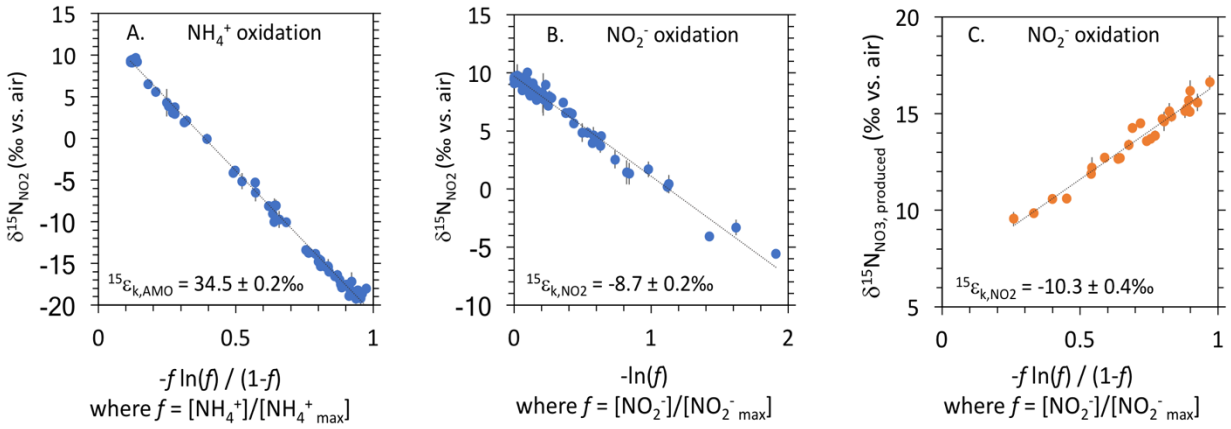

Figure 8. Rayleigh *fractionation for N isotope in NO_2^- and NO_3^-: $\delta^{15}N_{NO2}$ vs. f*ln(f)/(1-f) during NH_4^+ oxidation (A), $\delta^{15}N_{NO2}$ vs. ln (f) during NO_2^- oxidation (B), and $\delta^{15}N_{NO3}$ vs. f*ln(f)/(1-f) during NO_2^- oxidation (C). All 12 incubation bottles are represented. Kinetic isotope effects were calculated from the slopes of each line, according to the Rayleigh accumulated product equation for (A) and (B) and the Rayleigh substrate equation for (C). Error bars are analytical errors on individual measurements. Error on the $^{15}\varepsilon$ is error on the slope according to Type II linear regression.*

kinetic isotope effect on N during NH_4^+ oxidation. Indeed, a plot of highly resolved $\delta^{15}N_{NO2}$ from Experiment 2 and the Rayleigh product equation (Eq. 5; Fig 8A), yield an isotope effect ($^{15}\varepsilon_{k,AMO}$) of 34.5 ± 0.2‰. This value is relatively high in comparison with marine isolates but is concordant with freshwater bacterial isolates *Nitrosomonas europaea* and *Nitrosomonas eutropha* (Casciotti et al., 2003; Mariotti et al., 1981; Table 2). In turn, both substrate and product equations for a closed system Rayleigh model (Eqs. 5 and 8) provide estimates of kinetic N isotope effect for NO_2^- oxidation, where the substrate equation is:

$$\delta_{substrate} = \delta_{substrate,initial} - \varepsilon \times \ln(f) \quad (8)$$

Where *f* in both formulations is defined as $[NO_2^-]/[NO_{2\,max}^-]$. Equations 5 and 8 yield estimates of -10.3 ± 0.4‰ and -8.7 ± 0.2‰ (Fig. 8B and 8C), respectively. Although not identical, both values of $^{15}\varepsilon_{k,NO2}$ express inverse isotope fractionation during NO_2^- oxidation and are within the range observed in cultures (Buchwald and Casciotti, 2010; Table 2).

4.4 Implications for interpretation of NO_3^- isotopes in the environment ---

The observations in this study suggest that nitrification by freshwater community produces NO_3^- with an oxygen isotopic composition that reflects not only the source of O atoms, H_2O and O_2, but that it is also sensitive to large O-atom incorporation isotope effects and isotopic equilibration of NO_2^- with H_2O. Our results agree with analogous findings in other recent nitrification studies of sea water cultures and natural assemblage incubations (Buchwald et al, 2012) as well as forest soil incubations (Fang et al., 2012; Snider et al., 2010). Our

observed $\delta^{18}O$ values of nitrified NO_3^- at naturally occurring $\delta^{18}O_{H2O}$ were repeatedly lower than would be expected from just end-member contribution (Eq. 2). Therefore, assuming median values for O incorporation isotope effects, the only way that the $\delta^{18}O$ of nitrified NO_3^- could yields estimates as high as predicted by Eq. 2 at naturally occurring $\delta^{18}O_{H2O}$ would be if the $\delta^{18}O$ of ambient O_2 were highly elevated, and if there were little to no NO_2^- equilibration with H_2O. Elevated $\delta^{18}O_{O2}$ may be possible in highly respired soils with limited input of new O_2. Soil bacteria have been shown to respire O_2 with an isotope effect on the order of 20‰ (Lane & Dole, 1956). Assuming our values for O-atom incorporation isotope effects and no isotopic equilibration of NO_2^-, then ^{18}O enrichment of O_2 from respiration would have to increase the $\delta^{18}O_{O2}$ from 24.2‰ (equilibrium with the atmosphere) to ~ 60‰ in order to fortuitously conform to the $\delta^{18}O_{NO3}$ expected from Eq. 2 at a $\delta^{18}O_{H2O}$ of -5‰. In the event of NO_2^- equilibration, then the $\delta^{18}O$ of O_2 would have to be even heavier in order to yield $\delta^{18}O_{NO3}$ in the range predicted by Eq. 2.

The amount of NO_2^- exchange that may occur during nitrification is dependent on pH, temperature, nitrification rates, and the residence time of NO_2^-. The rate of abiotic exchange is pH and temperature dependent, such that rates are faster in more acidic, warmer waters. As in our experiments and other nitrification incubations (Buchwald et al., 2012; Snider et al., 2010) NH_4^+ oxidation and NO_2^- oxidation can become decoupled, thus allowing for high concentrations of NO_2^- to accumulate and increasing the amount of exchange that occurs. Snider et al. 2010 observed that the fraction of abiotic exchange in soils is inversely proportional to net nitrification rates, showing that slower rates allowed for more opportunity for exchange, even when NH_4^+ oxidation and NO_2^- oxidation were relatively coupled. However,

due to low concentrations and residence times of NO_2^- in the environment, and that significant abiotic equilibration can take weeks to months at near neutral pH (Buchwald & Casciotti, 2013), it is difficult to quantify how much abiotic exchange impacts the $\delta^{18}O$ of nitrified NO_3^-. Nevertheless, organism-catalyzed exchange seems likely to have a significant impact on the $\delta^{18}O$ of nitrified NO_3^-. Biologically mediated exchange during NH_4^+ oxidation has been found to be up to 26% for pure cultures of NH_4^+ oxidizers and closely coupled co-cultures (Buchwald et al., 2012; Karen L. Casciotti et al., 2010). A study of soil incubations found exchange to range from 37% in a temperate forest soil to 52% in a low organic matter agricultural soil with little NO_2^- accumulation (Snider et al., 2010). Interestingly, Snider et al., 2010 observed in one soil type at naturally occurring $\delta^{18}O_{H2O}$, the $\delta^{18}O$ of NO_3^- produced was similar to, and in some replicates greater than, what would be expected by Eq. 2. This may be possible if NO_2^- was almost fully exchanged and $^{18}\varepsilon_{k,H2O,2}$, which was not derived in this study, was at the lowest observed value in these particular incubations (~1‰; Buchwald et al., 2012). Conformity to Eq. 2 may be also be explained by potentially co-occurring denitrification, thus increasing the $\delta^{18}O$ of ambient NO_3^-, as some replicates of this soil type had $\delta^{18}O_{NO3}$ greater than predicted by Eq. 2. Nevertheless, most values for $\delta^{18}O_{NO3}$ from Snider et al., 2010 were lower than predicted by Eq. 2 by ~7‰ and when $\delta^{18}O_{NO3}$ produced was plotted against $\delta^{18}O_{H2O}$ (as in Fig. 5), the slopes were greater than 2/3 for all soil types, indicating that more than 2/3 of the O atoms in NO_3^- were derived from H_2O. Similarly, Fang et al., 2012 observed a range $\delta^{18}O$ NO_3^- produced by nitrification in temperate forest soils of -9.3 – 2.9‰, which were lighter than predicted by 5.2 – 9.5‰. They also saw an increasing trend between $\delta^{18}O_{NO3}$ and ground elevation, which they attribute to more NO_2^- exchange at elevation due the higher acidity of soils.

Instances where the $\delta^{18}O$ of nitrified NO_3^- is greater than predicted by Eq. 2 (Burns, 2002; Mayer et al., 2001; Spoelstra et al., 2007) have often been reported. For example, Mayer et al., 2001 reported $\delta^{18}O_{NO3}$ values for NO_3^- produced nitrification in acid forest floors to be up to 12‰ greater than predicted with a $\delta^{18}O_{H2O}$ of -8‰. The authors attributed the elevated $\delta^{18}O_{NO3,nitrified}$ value to the potential isotopic enrichment of O_2 from respiration and the possibility that "heterotrophic nitrification" imparts a high $\delta^{18}O$ on nitrified nitrate. While there is no a priori expectation that the reactions and catalyzing enzymes for nitrification by heterotrophs should differ from that by autotrophs, organic nitrogen compounds reportedly provide O atoms to NO_3^- during heterotrophic nitrification (Doxtrader, 1965; Focht and Verstraete, 1977; Wood 1988; Wood 1990), thereby eliminating any dependence of the $\delta^{18}O$ of NO_3^- on O_2, and possibly H_2O. Denitrification occurring simultaneously in anaerobic microsites of nitrifying soils was discounted as having any influence on the $\delta^{18}O_{NO3}$ in these studies because a simultaneous increase in $\delta^{15}N$ and $\delta^{18}O$ NO_3^-, indicative of denitrification (Lehmann et al., 2003; Sigman et al., 2005; Granger et al., 2008) was not observed. However, some workers have found that denitrification in ground water and soils can be significant, the impact of which has been under-estimated based on interpretation of NO_3^- isotopes in many systems (Houlton et al., 2006; Osaka et al., 2010), particularly as they can decouple N and O isotopes otherwise apparent for denitrification alone (Osaka 2010). Therefore, rather than the hypotheses put forth in these studies (Burns, 2002; Mayer et al., 2001; Spoelstra et al., 2007), we suspect that denitrification, co-occurring with nitrification, may cause the $\delta^{18}O$ of NO_3^- in some freshwater environments to fortuitously conform to, or be greater than predicted by Eq. 2.

Use of the fractional source contribution model estimate for $\delta^{18}O_{NO3}$, thereby ignoring kinetic isotope fractionation during O-atom incorporation and NO_2^- exchange with H_2O, can lead to an overestimation of nitrification as a source of NO_3^- in natural systems. We therefore sought an alternative model that could be used as a more accurate, but simple, representation of nitrified NO_3^- in the environment. We noticed that for all of our incubations with natural abundance H_2O, the $\delta^{18}O$ of final NO_3^- were all within a few ‰ of $\delta^{18}O_{H2O}$. All treatments in Experiment 1 were lighter than $\delta^{18}O_{H2O}$ by approximately 1‰, and treatments 1 and 2 for Experiment 2 were lighter by 2.2‰ and 1.4‰ respectively. In this vein, similar empirical correlates have emerged from studies of nitrifying cultures and from observations in marine systems: Buchwald et al. 2012 found the $\delta^{18}O$ of newly produced NO_3^- to consistently be within

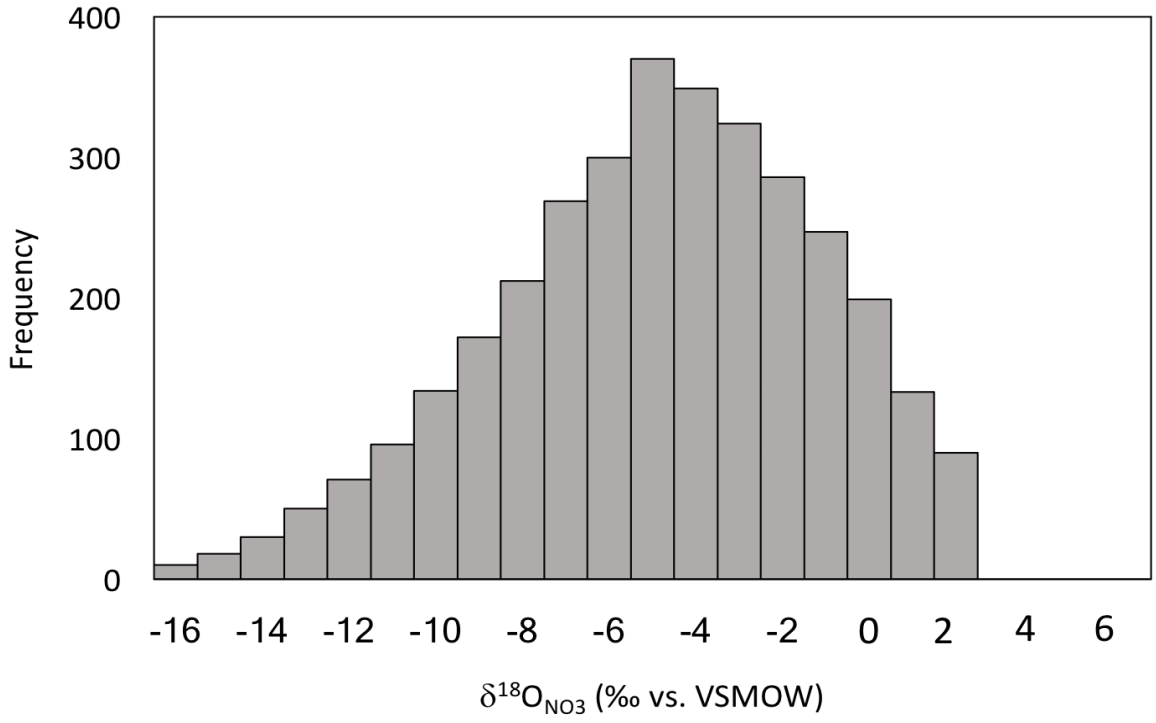

Figure 9. Density distribution of possible $\delta^{18}O$ NO_3^- values at a $\delta^{18}O$ H_2O of -5‰. Calculated from Eq.8 using varying O-incorporation isotope effects and exchange values that span the entire range observed in nitrifying cultures.

a few ‰ of $\delta^{18}O_{H2O}$. $\delta^{18}O$ values for nitrified NO_3^- close to that of H_2O are consistent with the expectation of remineralized NO_3^- in various marine systems (Casciotti et al., 2002; Granger et al., 2013; Rafter et al., 2013; Sigman et al., 2009), which have been used to interpret $\delta^{18}O_{NO3}$ in biogeochemical models (Casciotti et al., 2007; Sigman et al., 2005; Wankel et al., 2007). To test the hypothesis that $\delta^{18}O$ of NO_3^- produced by freshwater nitrification is close to that of H_2O, we created a density distribution of all plausible $\delta^{18}O_{NO3}$ produced at $\delta^{18}O_{H2O}$ = -5‰. Calculations of hypothetical $\delta^{18}O_{NO3}$ consisted of all permutations of (a) O-atom incorporation isotope effects covering the range observed in cultures, and (b) varying X_{NO2} at 0%, 25%, 50%, 75%, and 100% NO_2^- O-atom equilibration (Fig. 9). Of the 3,360 possible combinations of isotope effects and equilibration, over 60% were within ±3‰ of $\delta^{18}O_{H2O}$. Therefore, we propose that field studies of nitrification and NO_3^- source apportioning studies in freshwater environments take O-atom incorporation isotope effects and NO_2^- exchange into account by adopting the model that the $\delta^{18}O$ of nitrified NO_3^- is approximately equal to that of the $\delta^{18}O_{H2O}$. Although the O-atom incorporation isotope effects and amounts of NO_2^- exchange may vary widely from system to system, adoption of this convention will give a more accurate representation of the $\delta^{18}O_{NO3}$ produced by nitrification than that of 2:1 fractional source contribution.

4.5 Future Directions ---

Observations of $\delta^{18}O$ of NO_2^- and NO_3^- clearly show that the O isotope dynamics of stream water nitrification align with the model proposed by the Casciotti and Buchwald culture studies (Casciotti et al., 2010; Buchwald and Casciotti, 2010; Buchwald et al., 2012). Our study further provides evidence that the rule of thumb used as the expectation for nitrification in marine

systems, that $\delta^{18}O$ of nitrified NO_3^- is close to that of H_2O, is also applicable in freshwater systems. While some important aspects of freshwater nitrification have been resolved, some queries still remain undetermined, including: How much NO_2^- O atom exchange occurs in the environment, where NO_2^- concentrations and residence times are low? What governs organism- catalyzed exchange? How influential is the $\delta^{18}O$ of ambient O_2? With the answers to these questions, workers could ultimately arrive at the central question of: Can one reliably tease out the contribution of nitrification from other NO_3^- sources, such as atmospheric deposition and fertilizer, and from the influence of denitrification from NO_3^- N and O distributions in the environment?

References ---

Amberger, A., & Schmidt, H. L. (1987). Natürliche Isotopengehalte von Nitrat als Indikatoren für dessen Herkunft Author links open overlay panel. *Geochimica et Cosmochimica Acta*, *51*(10), 2699–2705.

Andersson, K. K., Philson, S. B., & Hooper, A. B. (1982). 18O isotope shift in 15N NMR analysis of biological N-oxidations: H2O-NO2-exchange in the ammonia-oxidizing bacterium Nitrosomonas. *Proceedings of the National Academy of Sciences*, *79*(19), 5871-5875.

Andersson, K. K., & Hooper, A. B. (1983). O2 and H2O are each the source of one O in NO-2 produced from NH3 by Nitrosomonas: 15N-NMR evidence. *FEBS Letters*, *164*(2), 236–240.

Böhlke, J.K., Mroczkowski, S.J., & Coplen, T.B. (2003). Oxygen isotopes in nitrate: New reference materials for 18O: 17O; 16O measurements and observations on nitrate-water equilibration. *Rapid Communications in Mass Spectrometry, 17(16), 1835-1846.*

Böhlke, J. K., Smith, R. L., & Hannon, J. E. (2007). Isotopic analysis of N and O in nitrite and nitrate by sequential selective bacterial reduction to N2O. *Analytical chemistry*, *79*(15), 5888-5895.

Braman, R. S., & Hendrix, S. A. (1989). Nanogram nitrite and nitrate determination in environmental and biological materials by vanadium (III) reduction with chemiluminescence detection. *Analytical Chemistry*, *61*(24), 2715-2718.

Buchwald, C., & Casciotti, K. L. (2010). Oxygen isotopic fractionation and exchange during bacterial nitrite oxidation. *Limnology and Oceanography*, *55*(3), 1064–1074.

Buchwald, C., Santoro, A. E., McIlvin, M. R., & Casciotti, K. L. (2012). Oxygen isotopic composition of nitrate and nitrite produced by nitrifying cocultures and natural marine assemblages. *Limnology and Oceanography*, *57*(3), 1361–1375.

Buchwald, C., & Casciotti, K. L. (2013). Isotopic ratios of nitrite as tracers of the sources and age of oceanic nitrite. *Nature Publishing Group*, *6*(4), 1–6.

Burns, D. A., & Kendall, C. (2002). Analysis of $\delta^{15}N$ and $\delta^{18}O$ to differentiate NO_3^- sources in runoff at two watersheds in the Catskill Mountains of New York. *Water Resources Research*, *38*(5).

Casciotti, K. L., Sigman, D. M., Hastings, M. G., Böhlke, J. K., & Hilkert, a. (2002). Measurement of the oxygen isotopic composition of nitrate in seawater and freshwater using the denitrifier method. *Analytical Chemistry*, *74*(19), 4905–4912.

Casciotti, K. L., Sigman, D. M., & Ward, B. B. (2003). Linking diversity and stable isotope fractionation in ammonia-oxidizing bacteria. *Geomicrobiology Journal, 20(4),* 335-353.

Casciotti, K. L., Böhlke, J. K., McIlvin, M. R., Mroczkowski, S. J., & Hannon, J. E. (2007). Oxygen isotopes in nitrite: Analysis, calibration, and equilibration. *Analytical Chemistry*, *79*(6), 2427–2436.

Casciotti, K. L. (2009). Inverse kinetic isotope fractionation during bacterial nitrite oxidation. *Geochimica et Cosmochimica Acta*, *73*(7), 2061–2076.

Casciotti, K. L., McIlvin, M., & Buchwald, C. (2010). Oxygen isotopic exchange and fractionation during bacterial ammonia oxidation. *Limnology and Oceanography*, *55*(2), 753–762.

Doxtrader K. G. (1965) Nitrification by heterotrophic microorganisms. Ph.D. thesis, Cornell University

Durka, W., Schulze, E. D., Gebauer, G., & Voerkelius, S. (1994). Effects of forest decline on uptake and leaching of deposited nitrate determined from (15) N and (18) O measurements. *Nature*, *372*(6508), 765.

Fang, Y., Koba, K., Makabe, A., Zhu, F., Fan, S., Liu, X., & Yoh, M. (2012). Low δ 18 O Values of Nitrate Produced from Nitrification in Temperate Forest Soils. *Environmental Science and Technology*, *46*(16), 8723–8730.

Focht D. D. and Verstraete W. (1977) Biochemical ecology of nitrifi- cation and denitrification. Adv. Mirob. Ecol. 1, 135–214.

Galloway, J. N., Dentener, F. J., Capone, D. G., Boyer, E. W., Howarth, R. W., Seitzinger, S. P., … Vörösmarty, C. J. (2004). *Nitrogen cycles: Past, present, and future*. *Biogeochemistry* (Vol. 70).

Garside, C. (1982). A chemiluminescent technique for the determination of nanomolar concentrations of nitrate and nitrite in seawater. *Marine Chemistry*, *11*(2), 159-167.

Gonfiantini, R., Stichler, W., & Rozanski, K. (1995). Standards and intercomparison materials distributed by the International Atomic Energy Agency for stable isotope measurements (No. IAEA-TECDOC--825).

Granger, J., Sigman, D. M., Prokopenko, M. G., Lehmann, M. F., & Tortell, P. D. (2006). A method for nitrite removal in nitrate N and O isotope analyses. *Limnology and Oceanography: Methods*, *4*(7), 205-212.

Granger, J., Sigman, D. M., Lehmann, M. F., & Tortell, P. D. (2008). Nitrogen and oxygen isotope

fractionation during dissimilatory nitrate reduction by denitrifying bacteria. *Limnology and Oceanography*, *53*(6), 2533–2545.

Granger, J., & Sigman, D. M. (2009). Removal of nitrite with sulfamic acid for nitrate N and O isotope analysis with the denitrifier method. *Rapid Communications in Mass Spectrometry*, *23*(23), 3753-3762.

Granger, J., Prokopenko, M. G., Mordy, C. W., & Sigman, D. M. (2013). The proportion of remineralized nitrate on the ice-covered eastern Bering Sea shelf evidenced from the oxygen isotope ratio of nitrate. *Global Biogeochemical Cycles*, *27*(3), 962–971.

Hollocher T. C. (1984) Source of the oxygen atoms of nitrate in the oxidation of nitrite by *Nitrobacter agilis* and evidence against a P-O-N anhydride mechanism in oxidative phosphorylation. *Arch. Biochem. Biophys.* **233,** 721–727.

Houlton, B. Z., Sigman, D. M., & Hedin, L. O. (2006). Isotopic evidence for large gaseous nitrogen losses from tropical rainforests. *Proceedings of the National Academy of Sciences of the United States of America*, *103*(23), 8745–50.

Kroopnick, K., & Craig, H. (1972). Atmospheric oxygen: isotopic composition and solubility fractionation. *Science*, *175*, 54–55.

Kumar, S., Nicholas, D. J. D., & Williams, E. H. (1983). Definitive 15N NMR evidence that water serves as a source of “O” during nitrite oxidation by Nitrobacter agilis. *FEBS Letters*, *152*(1), 71–74.

Lane, G. A., & Dole, M. (1956). Fractionation of oxygen iotopes during respiration. *Science*, *123*(3197), 574–576.

Lehmann, M. F., Reichert, P., Bernasconi, S. M., Barbieri, A., & McKenzie, J. A. (2003). Modelling nitrogen and oxygen isotope fractionation during denitrification in a lacustrine redox-transition zone. *Geochimica et Cosmochimica Acta*, *67*(14), 2529–2542.

Mariotti, A., Germon, J., Hubert, P., Kaiser, P., Letolle, R., Tardieux, A., & Tardieux, P. (1981). Experimental determination of nitrogen kinetic fractionation: some priciples; illustration for the denitrification and nitrification processes. *Plant and Soil*, *632*(1981), 413–430.

Mayer, B., Bollwerk, S. M., Mansfeldt, T., Hütter, B., & Veizer, J. (2001). The oxygen isotope composition of nitrate generated by nitrification in acid forest floors. *Geochimica et Cosmochimica Acta*, *65*(16), 2743–2756.

McIlvin, M. R., & Altabet, M. A. (2005). Chemical conversion of nitrate and nitrite to nitrous oxide for nitrogen and oxygen isotopic analysis in freshwater and seawater. *Analytical Chemistry*, *77*(17), 5589-5595.

McIlvin, M. R., & Casciotti, K. L. (2011). Technical updates to the bacterial method for nitrate isotopic analyses. *Analytical Chemistry*, *83*(5), 1850-1856.

Osaka, K., Ohte, N., Koba, K., Yoshimizu, C., Katsuyama, M., Tani, M., … Nagata, T. (2010). Hydrological influences on spatiotemporal variations of d15N and d18O of nitrate in a forested headwater catchment in central Japan: denitrification plays a critical role in groundwater. *Journal of Geophysical Research*, *115*, 1–14.

Rafter, P. A., Difiore, P. J., & Sigman, D. M. (2013). Coupled nitrate nitrogen and oxygen isotopes and organic matter remineralization in the Southern and Pacific Oceans. *Journal of Geophysical Research: Oceans*, *118*(10), 4781–4794.

Sigman, D. M., Casciotti, K. L., Andreani, M., Barford, C., Galanter, M., & Böhlke, J. K. (2001). A bacterial method for the nitrogen isotopic analysis of nitrate in seawater and freshwater. *Analytical Chemistry*, *73*(17), 4145–4153.

Sigman, D. M., Granger, J., DiFiore, P. J., Lehmann, M. M., Ho, R., Cane, G., & van Geen, A. (2005). Coupled nitrogen and oxygen isotope measurements of nitrate along the eastern North Pacific margin. *Global Biogeochemical Cycles*, *19*(4), 1–14.

Sigman, D., Karsh, K., & Casciotti, K. (2009). Ocean Process Tracers: Nitrogen Isotopes in the Ocean. *Encyclopedia of Ocean Sciences*, 4138–4153.

Silver, W. L., Lugo, A. E., Keller, M., Biogeochemistry, S., Mar, N., Silver, W. L., … Keller, M. (2017). Soil oxygen availability and biogeochemistry along rainfall and topographic gradients in upland wet tropical forest soils. *Biogeochemistry*, *44*(3), 301–328.

Snider, D. M., Spoelstra, J., Schiff, S. L., & Venkiteswaran, J. J. (2010). Stable oxygen isotope ratios of nitrate produced from nitrification: (18)O-labeled water incubations of agricultural and temperate forest soils. *Environmental Science & Technology*, *44*(14), 5358–64.

Spoelstra, J., Schiff, S. L., Hazlett, P. W., Jeffries, D. S., & Semkin, R. G. (2007). The isotopic composition of nitrate produced from nitrification in a hardwood forest floor. *Geochimica et Cosmochimica Acta*, *71*, 3757–3771.

Voerkelius, S., & Schmidt, H. L. (1990). Natural oxygen and nitrogen isotope abundances of compounds involved in denitrification. *Mitteilungen der Deutschen Bodenkundlichen Gesellschaft*, *60*, 361-366.

Wankel, S. D., Kendall, C., Pennington, J. T., Chavez, F. P., & Paytan, A. (2007). Nitrification in the euphotic zone as evidenced by nitrate dual isotopic composition: Observations from Monterey Bay, California. *Global Biogeochemical Cycles*, *21*(2), 1–13.

Weigand, M. A., Foriel, J., Barnett, B., Oleynik, S., & Sigman, D. M. (2016). Updates to instrumentation and protocols for isotopic analysis of nitrate by the denitrifier method. *Rapid Communications in Mass Spectrometry*, *30*(12), 1365-1383.

Wood P. M. (1988) Mono-oxygenase and free radical mechanisms for biological ammonia -oxidation. In *The Nitrogen and Sulphur Cycles*, Vol. 42 (ed. J. A. Cole and S. J. Ferguson), pp. 219–243, Cambridge University Press, Cambridge, New York.

Wood P. M. (1990) Autotrophic and heterotrophic mechanisms for ammonia oxidation. *Soil Use Manag.* **6,** 78–79

York (1966). Least-squares fitting of a straight line. *Canad. J. Phys.* 44: 1079-1086

York et al. (2004). Unified equations for the slope, intercept, and standard errors of the best straight line. *Am.J. Phys.* 72(3): 367-375.

Zhang, J. Z., Ortner, P. B., Fischer, C. J., & Moore, L. (1997). Determination of ammonia in estuarine and coastal waters by gas segmented continuous flow colorimetric analysis. *EJ Arar, Project Officer. Method*, *349*.

Zhang, J. Z., Ortner, P. B., & Fischer, C. J. (1997). Determination of nitrate and nitrite in estuarine and coastal waters by gas segmented continuous flow colorimetric analysis. *EPA Method*, *353*.